Charles University

Faculty of Science

Department of Biochemistry

Diploma thesis

The role of spliceosomal Prpf8 protein in DNA damage response pathways

Role sestřihového proteinu Prpf8 v buněčné odpovědi na poškození DNA

Bc. Andrea Bosáková

Supervisor: prof. RNDr. Marie Stiborová, DrSc.

Prague 2018

This thesis was carried out at the Institute of Molecular Genetics of the ASCR, v.v.i. Prague, 2016 - 2018.

Prohlašuji, že jsem tuto diplomovou práci vypracovala samostatně pod vedením školitelky prof. RNDr. Marie Stiborové, DrSc. a konzultantů doc. Mgr. Davida Staňka, Ph.D. a Mgr. Zuzany Cvačkové, Ph.D. Všechny použité prameny byly řádně citovány.

....

Místo a datum Podpis

Acknowledgements

My first thanks belong to Marie Stiborová who enabled me to work on this interesting project and who also gave me a lot of instructive advices and consultations.
I would like to thank David Staněk for accepting me to work in his great research group and for his kind leadership. I am very grateful for his professional as well as personal support. Special thanks go to Zuzka Cvačková for being such a patient and nice person. I am thankful for all advices that she gave to me. I have been working on this diploma thesis in a very professional and friendly environment and I would like to thank all members of our research group for that. My thanks also go to Jana Křížová who introduced me into the world of cell culture experiments, to Ivan Novotný, Anna Malinová and Zdeněk Cimbůrek who helped me with the microscope facilities that I was using and also to Libor Macůrek for his comments and advices.

Last but not least, I would like to thank all my friends and family for their support and kindness.

Abstract

RNA splicing is a process by which introns are removed from a pre-mRNA (precursor messenger RNA) and exons are joined to produce a mature mRNA. RNA splicing is performed by spliceosome, a large macromolecular complex that contains five small nuclear ribonuclear proteins (snRNPs) and more than 150 associated proteins. Recent structural studies showed that the U5 snRNP plays a central role in the spliceosome function and particularly the highly conserved U5 protein Prpf8 (pre-mRNA processing factor) that lies in the catalytic core of spliceosome.

Mutations in Prpf8 protein were connected to the disease known as retinitis pigmentosa (RP), which is one of the most common causes of retinal degeneration affecting 1 out of 4000 people worldwide. The major clinical manifestations of a typical RP are night blindness and tunnel vision. As the disease progresses, the peripheral visual field is further reduced, and patients lose central vision usually by the age of 60 years.

In this thesis we try to understand the mechanism underlying the pathogenesis of RP caused by mutations in Prpf8 protein.

Based on the data from literature, in which the authors present evidence that DNA damage triggers specific profound changes in late-stage spliceosome organization, we tested our hypothesis that the Prpf8 protein is involved in cellular response to DNA damage. We also used stable cell lines carrying RP mutations in Prpf8 protein to investigate the effect of these mutations on cellular DNA damage response.

Key words: RNA splicing, Prpf8 protein, retinitis pigmentosa, DNA damage response pathway

Abstrakt

Sestřih RNA je proces, během kterého jsou z pre-mRNA odstraněny introny a exony jsou spojeny za vzniku maturované mRNA. Sestřih pre-mRNA je katalyzovaný sestřihovým komplexem, spliceosomem, což je makromolekulární komplex tvořený pěti malými jadernými ribonukleoproteinovými proteiny (snRNPs) a více než 150 sestřihovými proteiny. Nedávné strukturální studie ukázaly, že U5 snRNP zastává zásadní roli ve spliceosomálním komplexu, zejména pak vysoce konzervovaný protein Prpf8, jenž tvoří jádro U5 snRNP a který je také považován za katalytické centrum celého spliceosomu.

Mutace v proteinu Prpf8 jsou dávány do spojitosti s onemocněním zvaným retinitis pigmentosa (RP), které představuje jednu z nejčastějších příčin degenerace buněk oční sítnice a které se vyskytuje celosvětově u 1 ze 4 000 lidí. Mezi hlavní klinické projevy tohoto onemocnění patří poruchy nočního vidění a tzv. tunelové vidění. S postupem času se také objevuje další snížení periferního vidění, což vede až k centrální ztrátě zraku, která se vyskytuje běžně do 60. roku života.

V této práci se snažíme porozumět mechanismu, kterým mutace v proteinu Prpf8 přispívají ke vzniku RP.

Na základě údajů uvedených v literatuře, ve které autoři předkládají důkaz, že poškození DNA způsobuje zásadní změny v pozdní fázi organizace spliceosomu, jsme se rozhodli testovat naši hypotézu, podle které by protein Prpf8 mohl být součástí buněčné odpovědi na poškození DNA. Využili jsme také stabilní buněčné linie nesoucí mutace spojené s RP v proteinu Prpf8, abychom zjistili, zda tyto mutace nějakým způsobem ovlivňují buněčnou odpověď na poškození DNA.

Klíčová slova: sestřih pre-mRNA, protein Prpf8, retinitis pigmentosa, buněčná odpověď na poškození DNA

Table of contents

1 THEORETICAL PART 12

1.1 SPLICING OF PRE-MRNA 12

1.1.1 SPLICEOSOME 12

1.1.2 SPLICING REACTIONS 13

1.1.3 ALTERNATIVE SPLICING 14

1.1.4 COMPOSITION OF THE SPLICEOSOME 15

1.1.5 U5 SNRNP 17

1.1.6 PRPF8 PROTEIN 18

1.2 SPLICING AND DISEASES 19

1.2.1 CIS-ACTING MUTATIONS 19

1.2.2 TRANS-ACTING MUTATIONS 20

1.3 CHROMATIN 23

1.4 DNA DAMAGE 25

1.4.1 ROLE OF HISTONE VARIANT H2AX IN DNA DAMAGE RESPONSE 26

1.5 DNA REPAIR PATHWAYS 29

2 AIMS AND OBJECTIVES 32

3 MATERIALS AND METHODS 33

3.1 MATERIALS 33

3.1.1 CHEMICALS 33

3.1.2 INSTRUMENTS 35

3.2 METHODS 35

3.2.1 CELL CULTURE 35

3.2.2 SIRNA INTERFERENCE 36

3.2.3 UV LIGHT/NEOCARZINOSTATIN (NCS) TREATMENT 37

3.2.4 CELLS FIXATION AND IMMUNOFLUORESCENCE 37

3.2.5 MICROSCOPY 38

3.2.6 PREPARATION OF CELL LYSATES 39

3.2.7 PROTEIN CONCENTRATION MEASUREMENT 39

3.2.8 SDS-PAGE AND WESTERN BLOT 40

3.2.9 DATA ANALYSING 42

4 RESULTS 43

4.1 UV LIGHT AND NCS ACTIVATES DIFFERENT DDR PATHWAYS 43

4.2 THE EFFICIENCY OF PRPF8 KD IN DIFFERENT CELL LINES 44

4.3 KDOF PRPF8 DOES NOT AFFECT THE LEVEL OF γH2AX HISTONE 46

4.4 KD OF PRPF8 PROTEIN INFLUENCES THE LEVEL OF γH2AX IN HELA CELLS AFTER UV LIGHT IRRADIATION 47

4.5 RP MUTANTS SHOW DIFFERENT RESPONSE TO DNA DAMAGE 50

4.6 DOWN REGULATION OF PRPF8 PROTEIN DOES NOT AFFECT THE LEVEL OF γH2AX AFTER THE NCS TREATMENT 54

4.6.1 DETERMINATION OF NCS CONCENTRATION IN HELA CELLS 54

4.6.2 THE CELLULAR RESPONSE TO DNA DAMAGE CAUSED BY NCS 55

5 DISCUSSION 59

6 CONCLUSION 63

7 REFERENCES 64

Abbreviations

AB	antibody
$[pY]_n$	polypirimidine tract
AP-site	apurinic/apyrimidinic site
APS	ammonium persulfate
AS	alternative splicing
ATM	ataxia telangiectasia mutated
ATP	adenosine triphosphate
ATR	ataxia telangiectasia mutated related
ATRIP	ataxia telangiectasia mutated related interacting protein
BAC	bacterial artificial chromosome
BCA	bicinchoninic acid
BER	base excision repair
bp	base pair
BSA	bovine serum albumin
Chk2	checkpoint kinase 2
Da	Dalton
DDR	DNA damage response
DMEM	Dulbecco's Modified Eagle Medium
DNA	deoxyribonucleic acid
DNA-PK	DNA-dependent protein kinase
dsDNA	double stranded DNA
EDTA	ethylenediaminetetraacetic acid
EGTA	triethylene glycol diamine tetraacetic acid
F	phenylalanine
FBS	fetal bovine serum
GFP	green fluorescent protein
H2A/B	histone H2A/B
H2AX/Z	histone H2AX/Z
H3	histone H3
H4	histone H4
HR	homologous recombination

HRP	horseradish peroxidase
IF	immunofluorescence
Jab1	c-Jun activation domain binding protein 1- like
KD	knock down
LAP	localization and affinity purification
MMR	mismatch repair
mRNA	messenger ribonucleic acid
N	asparagine
NA	numerical aperature
NC1	negative control 1
NCS	neocarzinostatin
NER	nucleotide excision repair
NHEJ	non-homologous end joining
NLS	nuclear localization signal
NTD1 /2	N-terminal domain 1/2
PAGE	polyacrylamide gel electrophoresis
PBS	phosphate buffered saline
PFA	paraformaldehyde
PI3K	phosphatidylinositol-3-kinase
PIPES	piperazine-N,N′-bis(2-ethanesulfonic acid)
pre-mRNA	precursor messenger ribonucleic acid
PTMs	post-translational modifications
RH	RNase-H-like
RNA	ribonucleic acid
RP	retinitis pigmentosa
RPA	replication protein A
RPE	retinal pigment epithelium
RT/En	reverse transcriptase-like/endonuclease-like
S	serine
SEM	standard error of the mean
Ser317	serine 317
siRNA	small interfering ribonucleic acid
SMA	spinal muscular atrophy

SMN1/2	survival of motor neuron 1/2
snRNA	small nuclear ribonucleic acid
snRNP	small nuclear ribonuclear protein
ssDNA	single-stranded DNA
TEMED	tetramethylethylenediamine
TMG	2,2,7- trimethylguanosine
U	uridine
UTR	untranslated region
UV	ultraviolet
WB	western blot
WT	wild type
WT1 gene	Wilm's tumor gene
Y	tyrosine
γH2AX	phosphorylated histone H2AX variant

1 Theoretical Part

1.1 Splicing of pre-mRNA

The splicing of nuclear pre-mRNA is an essential process by which introns (long intervening sequences) are removed from a pre-mRNA and exons (coding sequences) are ligated together to produce a mature translatable mRNA. The phenomenon of "split genes" was first described in 1977 and it enabled to understand why the RNA found in nucleus is so much longer than the RNA in cytoplasm.[1] Nowadays, it is known that an average human gene contains 8.8 exons and 7.8 introns. The average length of exon in around 300 base pairs (bps) and the length of intron varies around 3.5 kbp.[2]

1.1.1 Spliceosome

RNA splicing is performed by spliceosome, a large macromolecular complex that contains five small nuclear ribonuclear proteins (snRNPs) and more than 150 associated proteins.[3] The vast majority of introns are spliced by a major spliceosome that is composed of U1, U2, U4, U5 and U6 snRNPs. Beside that, there is also a minor spliceosome that removes a minor class of introns by closely related machinery containing U11, U12, U4atac, U5 and U6atac snRNPs. Although the four snRNPs are specific to the minor splicosome, the U5 snRNP is shared by the minor and major splicosome.[4]

Spliceosome recognizes the exon/intron boundaries mainly by base pairing with the specific sequence elements. Essential elements include the 5' splice site, the branch point, the polypyrimidine tract and the 3' splice site (see Fig. 1 on page 13). Metazoan pre-mRNAs contain two classes of introns that are distinguished by their specific splice site sequences and their removal by the different spliceosomal type. Introns that are excised by the major spliceosome are known as U2-type introns and they contain the canonical GT-AG intron boundaries. The second type of introns is spliced by the minor spliceosome and it is known as U12-type. Only 0.5 % of all the human introns contains non-canonical intron/exon boundaries and are catalyzed by the minor spliceosome, therefore the canonical and dominant human splicing will be discussed in this thesis.[1 5]

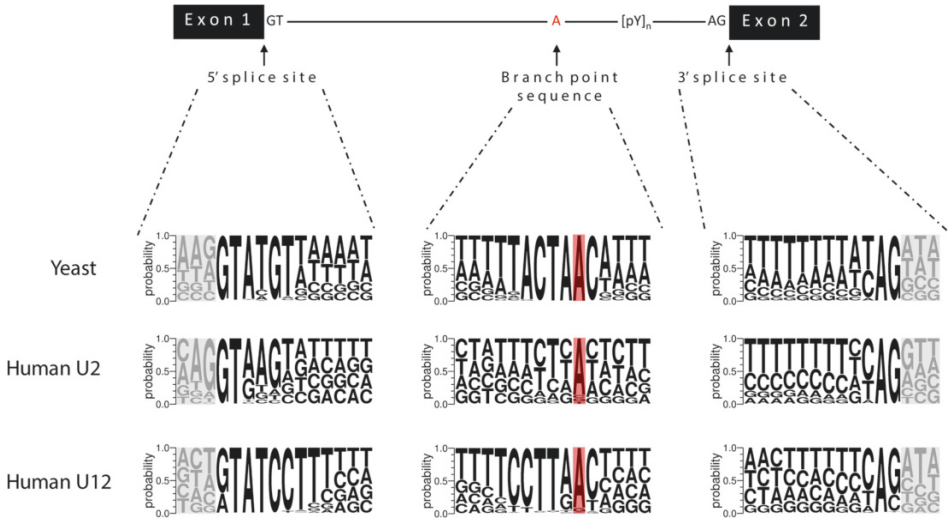

Fig. 1: The essential splicing elements
Splicing elements in pre-mRNA include 5' splice site, branch point, polypyrimidine tract and 3' splice site. Consensus sequences for individual elements were generated by WebLogo 3. [6]
In the human U2-type introns contain predominantly GT-AG termini.
The non-canonical human U12-type introns contain AT-AC termini, however subsequent genomic analysis showed that the GT-AG termini are more frequent.
Grey boxes represent exonic regions, red boxes represent the branch point adenosine and the $[pY]_n$ indicates the polypyrimidine tract.
Taken from [5]

1.1.2 Splicing reactions

Nuclear pre-mRNA splicing involves two isogenic transesterification steps that require ATP, $MgCl_2$ and monovalent cations to remove the intron and form the protein-coding mRNA.

In the first step of spliceosome assembly, the U1 snRNP engages with the 5' splice site and associated proteins help the U2 snRNP bind to the branch point sequence to generate complex A (see Fig. 2 on page 14). In the following step, the preassembled U4/U6.U5 tri-snRNP is recruited to form an inactive complex B. At this point, the U1 and U4 snRNP are released and the catalytically active complex B^* is formed. After rearrangement, the U6 snRNP binds the 5' splice site and also associates with the U2 snRNA that promotes the first catalytic step to begin. In this transesterification reaction, the 2' OH group of the conserved branch point adenosine performs a nucleophilic attack at the phosphate group of the 5' splice site and cleaves the phosphodiester bond. This step leads to releasing the 5' exon and the intron lariat intermediate is created. This reaction also forms the complex C.[5 7]

Finally, in the complex C, the second catalytic step proceeds by the nucleophilic attack of the 3' OH group of the detached exon at the phosphate group of the 3' splice site to excise the intron lariat and to ligate the 5' and 3' exon together.

During the mRNA processing spliceosome undergoes a number of structural rearrangement that are important for the right assembly. After every "splicing round" the snRNPs are recycled.[1 5]

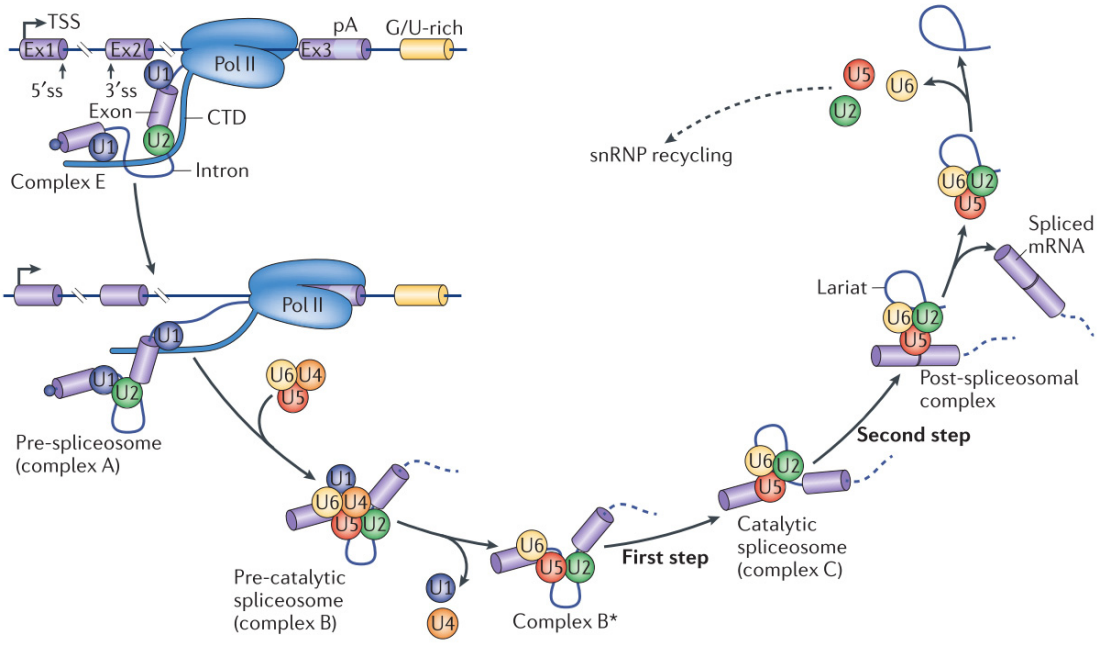

Fig. 2: The pathways of spliceosomal assembly
Spliceosome catalyses the two-step intron removal from pre-mRNA.
Taken from [7]

1.1.3 Alternative splicing

Alternative splicicng (AS) is a process in which a single gene may create different versions of mRNA, called isoforms. Individual mRNA isoforms encode different proteins and help to expand the proteome coding potential of genes.[8]

AS is a deviation from the constitutive splicing and it includes various types of "alternative splicing events" such as exon skipping (cassette exon), mutually exclusive exon, intron retention, mutually exclusive 5' untranslated regions (UTRs), mutually exclusive 3' UTRs, alternative 5' splice sites and alternative 3' splice sites (see Fig. 3 on page 15).[9]

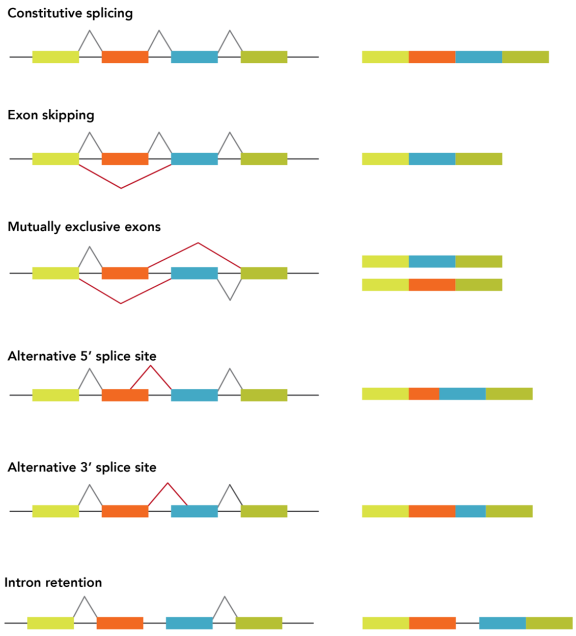

Fig. 3: Scheme of typical alternative splicing events compared to constitutive splicing
Taken from[10]

A lot of studies have shown the fundamental role of AS across biological systems. The species of higher eukaryotes have been discovered to exhibit a higher proportion of alternatively spliced genes, which underlays the importance of AS in evolution. In human organism, AS occurs in more than 95 % genes and it mediates diverse biological processes over the entire life span. Different mRNA isoform production plays a critical role in tissue development and also in cellular responses to various stimuli therefore the activity of AS is highly regulated. There have been described two main categories of elements that regulate the pre-mRNA splicing and act as antagonists- the silencers, that inhibit splicing, and the enhancers, that promote splicing. Both of them can be located either in exonic or intronic region of pre-mRNA and their activity is controlled by number of associated proteins.[11]

1.1.4 Composition of the spliceosome

Spliceosome is a macromolecular complex assembled from five snRNPs- U1, U2, U4, U5 and U6. These splicing components contain uridine-rich small nuclear RNA (U-rich snRNA) and associated proteins. Biogenesis of snRNPs is a multi-compartmental process that is essential for a proper splicing and cell fate.

1.1.4.1 Uridine-rich small nuclear RNA

The key component of each snRNP particle is a U-rich non-coding RNA found in a nucleus of eukaryotic cells. This type of nuclear RNA is approximately 100-200 nucleotides long and it may occur in various isoforms. Based on the structure, sequences and associated proteins, snRNAs have been divided into two classes (see Fig. 4).[12]

The first class is known as the Sm-snRNAs and it includes the U1, U2, U4 and U5 snRNAs that are transcribed by RNA polymerase II. Characteristic features of the mature Sm-class of snRNAs is a 2,2,7- trimethylguanosine (TMG) cap that is found at the 5' end, a 3' stem loop and a specific Sm binding region.[13] The 5' cap serves as a signal for an export of snRNPs from the nucleus into the cytoplasm where the heptameric Sm-ring is assembled around each snRNA to stabilize its structure. After the ring is formed, the snRNP is exported back to the nucleus, particularly into Cajal bodies where the further biogenesis of snRNPs takes place. Mature snRNPs are stored within compartments known as nuclear speckles.[14 15]

The second class of snRNAs is known as the LSm-class and it includes only the U6 snRNA that is transcribed by RNA polymerase III. U6 snRNA possess a 5' monomethyl-phosphate cap and a 3' polyuridine binding site for LSm-proteins. During maturation, La protein is associated with U6 snRNA to stabilize and protect the structure. It is also used as a signal that guides the snRNP into the nucleolus where further modifications take place. After the main modifications are finished, the La protein is released and the heptameric LSm-ring is formed around the 3' end site. After further alternations, the U6 snRNP is transported into the Cajal bodies where it joins the rest of snRNPs.[15 16]

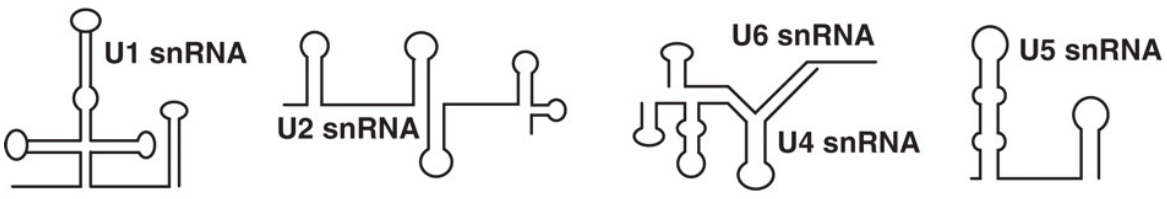

Fig. 4: Different structures and shapes of snRNAs
Modified from[17]

1.1.4.2 Spliceosomal proteins

Spliceosomal machinery contains around 150 proteins that dynamically join or leave splicing reactions. Beside the Sm and LSm proteins, there are snRNP specific

proteins that form the particles (see Fig. 5) and also associated proteins that help the large complex to work.

In this project, we focused on the Prpf8 protein that is a part of U5 snRNP and therefore this particle will be discussed individually.

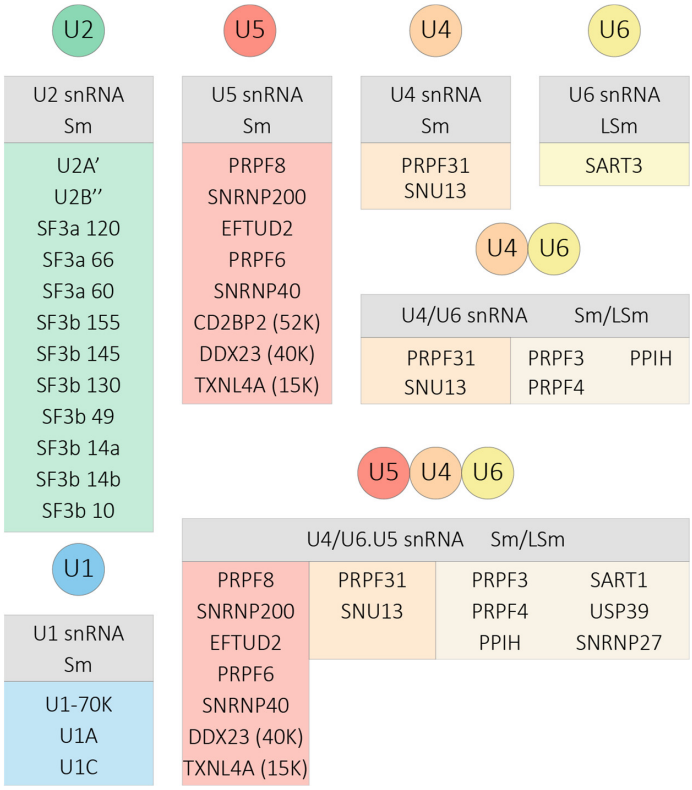

Fig. 5: Overview of snRNP specific proteins in inactive complex B
Each snRNP is composed of the core proteins (grey) and specific proteins (colourful)
Taken from[18]

1.1.5 U5 snRNP

U5 snRNP plays an essential role in pre-mRNA splicing in which it catalyses both transesterification reactions. In absence of functional U5 snRNP the spliceosome assembly cannot be proceed and the splicing is inhibited.

The composition of U5 particle is very dynamic depending on a particular step in spliceosome assembly. Apart of the Sm proteins, stable components of the particle are proteins Prpf8 (220 kDa), Brr2 (200 kDa) and Snu114 (116 kDa).[19] As the U5 snRNP is matured, another additional proteins join the particle to create 20S U5 snRNP. In the next step, U5 particle is brought together with the U4/U6 di-snRNP and the structure is

reorganized to produce the 25S U5 snRNP that is a part of the U4/U6.U5 tri-snRNP. The bridging between the particles is due to the Prpf6 protein that connects the particles. The main rearrangement of the U5 particle occurs during the activation of complex B, in which number of proteins dissociates from the complex and other non-snRNP proteins are recruited. As the splicing is finished, the 35S U5 snRNP is released with many additional proteins and splicing factors attached. Before the next round of splicing, the U5 snRNP is recycled, however the mechanism stays still unclear. [20] [21]

1.1.6 Prpf8 protein

Prpf8 (also known as hPrp8 or Prp8) protein is a highly conserved component of U5 snRNP and U4/U6.U5 tri-snRNP. Prpf8 protein is conserved in both in its sequence and its size which varies between 220 kDa and 280 kDa depending on the organism.[22] Mouse Prpf8 protein, for example, differs by only three amino acids residues from the human ortholog and the sequence identity from yeast to human reaches 61 %. The importance of Prpf8 protein is highlighted by the fact that functional Prpf8 protein is required in each tissue, however its expression is higher in skeletal and cardiac muscle tissue. The Prpf8 protein is coded by one gene containing 42 exons.

Prpf8 protein contains a number of motifs (from N to C terminus): NTD1 (N-terminal domain 1), NTD2 (N- terminal domain 2), RT (reverse transcriptase-like)/En (endonuclease- like) domain, RH (RNase H- like) domain and Jab1 (c-Jun activation domain binding protein 1- like) domain (see Fig. 6 on page 19).[23] Recently, a nuclear localization signal (NLS) was described within the NTD1 domain.[24]

As the major protein of the catalytic active U5 snRNP, the Prpf8 protein is involved in many interactions. UV-crosslinking experiments have shown that Prpf8 protein interacts with 5' splice site, 3' splice site and with branch point sequence in a pre-mRNA. Beside pre-mRNA, Prpf8 protein also interacts with other proteins that are part of the U5 snRNP, particularly with Prpf6 protein, Brr2 and Snu114. The Brr2 is an ATP-dependent helicase that is involved in unwinding the U4/U6 di-snRNP during spliceosome assembly. Activity of this helicase is regulated by Snu114 protein and by binding to the Jab1 domain of Prpf8 protein. Recent studies have discovered another assembly factor named Aar2 that also interacts with Prpf8 protein and also participates in biogenesis of the U5 snRNP. Additionally, immunoprecipitation experiments showed interaction between U5 snRNP

(U4/U6.U5 tri-snRNP) and RNA polymerase II. That evidence supports the coupling of pre-mRNA splicing with the pre-mRNA synthesis by RNA polymerase II. [25]

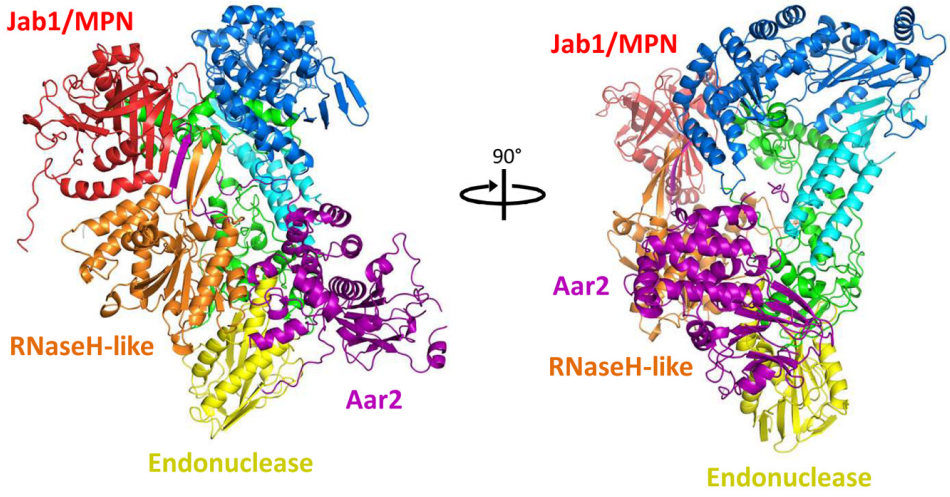

Fig. 6: Domain structure of Prpf8 protein associated with Aar2
The scheme shows the Jab1/MPN domain, the RNaseH-like domain and the Endonuclease domain that interact with the Aar2 protein
Modified from[26]

1.2 Splicing and diseases

As it was described above, pre-mRNA splicing plays a crucial role in basically all human cells and therefore it is obvious that mutations altering splicing cause various disorders. There are two main categories that classify mutations altering splicing-mutations in sequence that determines splicing (*cis*-acting mutations) and mutations in basal spliceosome machinery (*trans*-acting mutations).[27]

Mutations that affect pre-mRNA splicing account from at least 15 % disease-causing mutations with up to 50 % of all described mutations.[28]

1.2.1 Cis-acting mutations

Cis-acting mutations occur in sites important for pre-mRNA splicing (5' splice site, branch point, polypyrimidine tract, 3' splice site, enhancer and silencer region) and may affect the use of these sites. Disruption of splicing can result in a total loss of gene expression, however more common is a shift in natural ration between various isoforms of one gene, or an introduction of a miss-spliced isoform. [27]

Wilm's tumor gene (WT1) is an example of disruption of alternatively spliced isoforms due to a mutation. The mutation causes elimination of one of the 5' splice site leading to the loss of one WT1 isoform. Lack of the isoform has been linked to disease known as Frasier's syndrome, a developmental disorder affecting mainly kidney and gonad.[29] Cis-acting mutations have been also connected to a cancer promotion. Some of the incorrectly spliced genes may be part of cell-growth regulation systems and any deviation in this process has fatal consequences. [30]

1.2.2 Trans-acting mutations

Trans-acting mutations occur in spliceosomal proteins and factors that regulate splicing. While cis-acting mutations affect mostly a single gene, mutations in spliceosomal components create the potential to multiple genes to be miss-spliced. Many of somatic trans-acting mutations have been identified by comparison of sequence from cancerous and healthy tissues.[27]

1.2.2.1 Spinal muscular atrophy

Spinal muscular atrophy (SMA) is an autosomal recessive neuromuscular disorder that affect 1 out of 6 000 - 10 000 live births.[31-32] Symptoms and clinical manifestation of the SMA varies depending on the specific SMA type and stage of disease, however the common feature is a gradual degeneration of motor neurons in the spinal cord and consequent skeletal muscle atrophy that leads to death in early childhood. Almost 95 % of all SMA cases are caused by mutations in SMN1 (Survival of motor neuron 1) gene that is located on the fifth chromosome. Beside the SMN1 gene, cells also encode the SMN2 gene and its sequence differs only in a few nucleotides that are a cause of alternative splicing resulting in expression of a shorter SMN isoform (80-90 %) and the full-length product is in only 10-20 % of all transcripts. SMN protein is essential for Sm-ring formation and it was also found in Cajal bodies, suggesting it takes part in biogenesis of snRNPs. Once, the SMN1 gene is mutated, the SMN2 protein compensates the loss. The amount of the SMN2 protein, particularly the full-length version of SMN2 protein is related to a SMD type and also to prognosis. [33]

1.2.2.2 Retinitis Pigmentosa

Retinitis Pigmentosa (RP) is a hereditary retinal degenerative disorder affecting 1 out 4000 individuals, without any apparent link to ethnic or racial background. It causes progressive degeneration of photoreceptor cells, including rods and cones, and it also affects retinal epithelium (RPE) cells, which create another layer of the retina. Rod cells are concentrated in the outer edge of retina and they are responsible for peripheral and low-light vision (scotopic vision). Cone cells, on the other hand, are responsible for sharp, central and colour vision and function better in relative bright light. In general, rods are more sensitive to light than cones and in case of RP rods are affected earlier and more critically. The loss of photoreceptor cells leads to RPE cells migration. RPE cells are then accumulated close to retinal vessels where they form a characteristic pigment deposit known as bone spicules. The bone spicules is a hallmark of RP disease and it occurs in areas of retina in which photoreceptors are missing (see Fig. 7). Typical symptoms of RP are characterized by decreased night vision and excessive light sensitivity that is caused by rod cells degradation. As the disease progresses the peripheral visual field is reduced and the cone cells are also affected resulting in reduction of visual acuity and impairments in colour vision. Eventually, total blindness ensue, however not all patients reach to this point. Beside the typical form of RP, there is also RP known as cone-rod dystrophy in which cones are affected earlier that rods and it causes a different disease progression.[34]

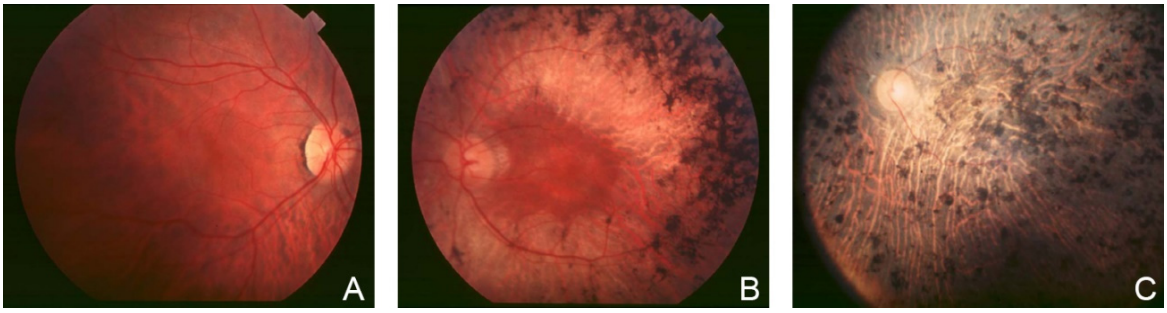

Fig. 7: Scheme of retina of RP patients
a) fundus of early stage of RP patient b) fundus of mid stage of RP- bone spicules is visible c) fundus of late stage of RP- the pigment deposits are accumulated all over the retina, vessels are attenuated
Modified from [34]

RP displays all three patterns of Mendelian inheritance- autosomal recessive (50-60 % of cases), autosomal dominant (30- 40 % of cases) and X-linked (5- 15 % of cases)

pattern. Genetic studies have identified around 150 genes associated with the RP and most of them are expressed pre-dominantly in retina.

Beside the retina specific genes, another six genes encoding proteins that participate in regulation of transcriptional and posttranscriptional modifications of genes, were associated with RP. Proteins produced specifically in retina are involved mostly in processes like retina cell signalling, vitamin A metabolism, photo transduction and structural organization of photoreceptors. [35]

Mutations in genes affecting pre-mRNA splicing have been found in six genes related to U4/U6.U5 tri-snRNP architecture, namely in Prpf31, Prpf6, Prpf8, Prpf4, Prpf3, and Brr2, and in two genes encoding non-snRNP spliceosomal proteins: PAP1 and DHX38. The molecular mechanism by which mutations in splicing factors that are expressed in most of the human cells cause retina specific disease remains unclear. It also remains speculative why only tri-snRNP specific genes are affected. Several hypotheses have been proposed explaining this phenomenon. It is likely that retina-specific cells have higher demands on pre-mRNA splicing comparing to other cells. This hypothesis also corresponds with the fact that retina cells have one of the most active metabolism which is demonstrated by an increased number of mitochondria in photoreceptors. [18 36 37]

1.2.2.3 The role of Prpf8 protein in Retinitis Pigmentosa

Eleven missense mutations causing amino acid substitutions were identified in the PRP8 gene and have been connected to autosomal dominant RP. All of the RP mutations occur at different positions within the C-terminal Jab1 domain. This domain is mainly responsible for binding and regulation of the Brr2 helicase. However the entire Jab1 domain strongly stimulates Brr2 activity, the C-terminal tail is inserted into the active site of Brr2 and it sterically inhibits its activity. Consistently, RP mutations that were found in the very C-terminus part of the protein increase the helicase activity, probably by removing the inhibitory region. Concurrently, RP mutations found toward the C-terminal Jab1 domain have been shown to weaken the Prpf8-Brr2 interaction and to have a negative effect on helicase stimulation.[20 38 39 40 41]

The connection between mutations in PRP8 gene and RP has been studied mostly in yeast providing findings that were used for further research in mammalian organisms. In yeasts, the RP mutations affecting the Jab1 domain of PRP8 were divided into three groups.[39] The first group includes RP mutations that were found within the globular region

of Jab1 domain (residues up to 2309) affecting the fold stability of the protein. Mutations in this region significantly influence splicing efficiency and show the strongest assembly defects. The protein instability is also manifested by faster degradation of the protein and by increased cytoplasmic localization comparing to mutants from another groups. Available clinical data correlates with the observation in yeasts and shows that patients carrying group I mutations suffer from more progressive type of RP.[42] The strongest phenotype was described in S2118F mutation that may be connected to its unique location outside of exon 42, comparing to another RP mutations, S2118F residue occurs in a distal region from C-terminus tail.[43]

RP mutations in the proximal part of the C-terminal tail of Jab1 domain (residues 2310- 2314) represent the second group influencing the interaction with Brr2 helicase. The third group of RP mutations includes the distal region of the C-terminal tail of Jab1 domain (residues 2315- 2336) and it is characterised by regulation of Brr2 helicase activity. [39] [44] The group III mutation Y2334N is located at the end of the C-terminal part and according to previous results it may inhibit the unwinding activity of the Brr2 helicase. In contrast to S2118F residue, this mutation does not affect formation of the U5 snRNP, neither the tri-snRNP formation, however it affects the splicing efficiency (see Fig. 8).[43]

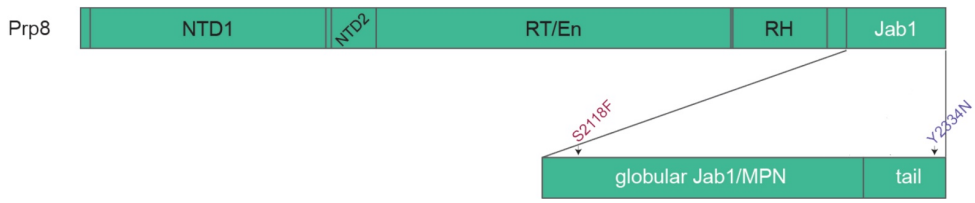

Fig. 8: Positions of RP mutations in Prpf8 sequence

1.3 Chromatin

DNA in eukaryotic organisms is enclosed in a cell nucleus that occupies more than 10 % of the cell volume in an average mammalian cell. Considering the total length of DNA in every cell of human body, it is obvious that DNA must be packed into a compact shape. To be more accurate: the haploid human genome contains approximately 3 billion base pairs (bps) of DNA, considering that most of the cells carry two copies of each chromosome (except of germ cells) that makes 6 billion bps of DNA per one cell. Because

each base pair is around 0,34 x 10^{-9} m long, each diploid cell contains around 2 meters of DNA.[45]

The compact shape of DNA in nucleus is achieved via the dynamic nucleoprotein organisation of eukaryotic DNA into chromatin. The basic unit of chromatin is called nucleosome, which contains 147 bps DNA wrapped 1.7 times around an octamer of histones- specialized basic proteins that bind and fold DNA- generating numbers of coils and loops. This octamer consists of two molecules of each core histone H2A, H2B, H3 and H4 (see Fig. 9).[46]

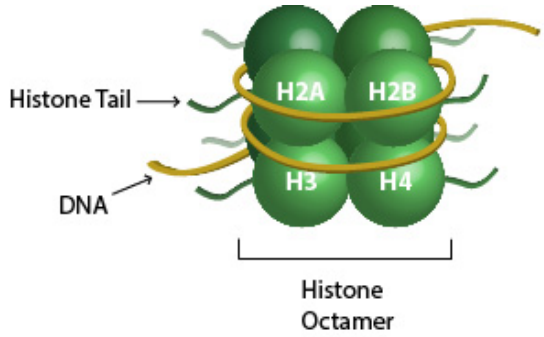

Fig. 9: The histone octamer structure.
The core of histone octamer contains two H2A histones, two H2B histones, two H3 histones and two H4 histones. DNA (147 bps) is wrapped around the histone octamer to create a nucleosome.
Modified from [47]

Despite the high conservation of the core histones, eukaryotic organisms produce also non-canonical histones, which differ in amino acid sequence from the canonical histones. Multiple histone variants and chemical modifications of histones contribute to the diversity of chromatin structure. The chromatin structure depends mainly on the cell cycle state, for example: during the interphase chromatin is loose to be more accessible for enzymes involved in DNA replication, transcription or repair, this structure is called *euchromatin.* In contrast, we recognize a highly condensed and compacted structure known as *heterochromatin,* which contains mostly inactive genes. The loosening or condensation which is performed by remodeling enzymes, allow a cell to regulate its gene expression.[45]

Gene expression is also regulated by many histone covalent modifications, including acetylation, the mono-, di-, and tri- methylation and the phosphorylation. However, most of the modification events take place at the positively charged N-terminal histone tails that are poorly structured and protrude from the nucleosome, some of the modifications also occur on the globular histone core. [48] Chromatin structure is not

important only for regulation of gene expression but it also helps during mitosis and prevents DNA damage events. [49]

1.4 DNA damage

Genome stability and integrity in eukaryotic cells are constantly threatened by a number of exogenous as well as endogenous factors. It has been estimated that an individual cell can suffer up to one million mutations per day, which generates more than 10^{18} DNA errors in human body per day. Since the genome integrity is essential for life, cells have evolved a highly organized network of cellular pathways that sense, signal and repair DNA lesions. This network is also known as DNA damage response (DDR) pathway and it uses signal sensors, transducers and effectors as a typical signal transduction pathway. DDR regulates events such as cell-cycle arrest, apoptosis and it also controls the activation of DNA repair mechanisms (see Fig.10).[50]

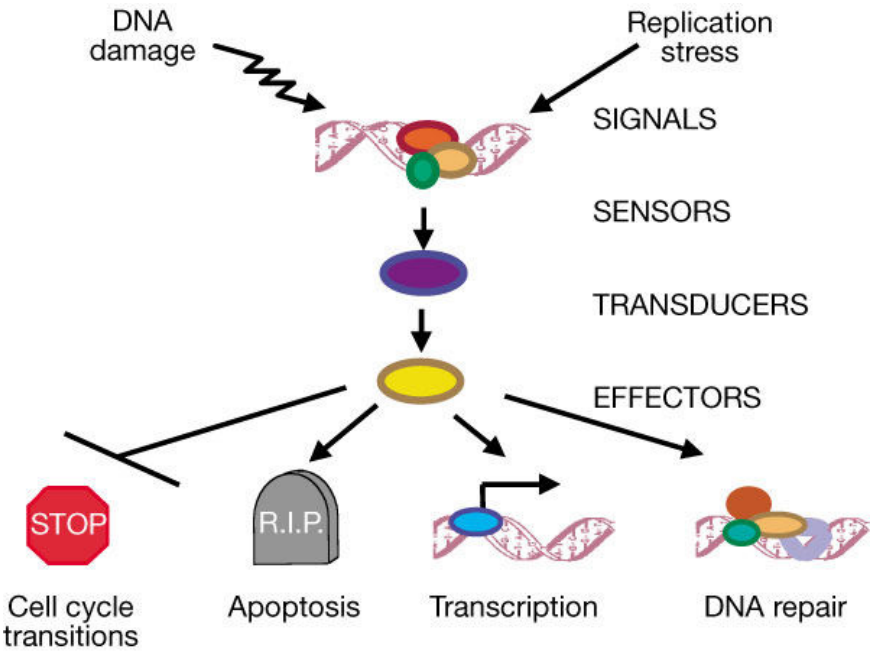

Fig.10: The DNA damage response network
After DNA damage the signal molecules are recognized by sensors that pass the message on transducers that activate the effectors. The DDR can lead to different events such as cell cycle arrest, apoptosis, alteration of transcription or DNA repair.
Taken from [51]

Endogenous sources of DNA damage such as oxidant agents, produced by cellular metabolism or defects in DNA replication may lead to hydrolysis, oxidation, alkylation

and mismatch of DNA bases. The frequency of DNA lesions is even more increased when cells are exposed to exogenous genotoxic agents such as UV light, ionizing radiation or toxic chemicals. As there is a wide variety of DNA lesions, cells have evolved numbers of DNA repair mechanisms that remove DNA damage.

1.4.1 Role of histone variant H2AX in DNA damage response

Histone modifications play fundamental roles in most biological processes that are involved in the manipulation and expression of DNA. There are plenty of post-translational modifications (PTMs), especially on the histone tails, that have very different consequences, however all of them are carefully regulated (see Fig. 11). During the PTMs specific molecules, known as effectors, bind to DNA and interpret the signal, eventually leading to another event.[52]

One of the most common PTM is a histone phosphorylation, which takes place on serines, threonines or tyrosines, predominantly, but not exclusively, in the N-terminal tails of all the four histones and C-terminal domains of histone H2A and H2B. This process is modulated by many specific enzymes known as kinases and phosphatases that act only on one or a few sites on histone tails. All of the known kinases transfer phosphate group from ATP to the hydroxyl group of target amino-acid side chain.[52] [53]

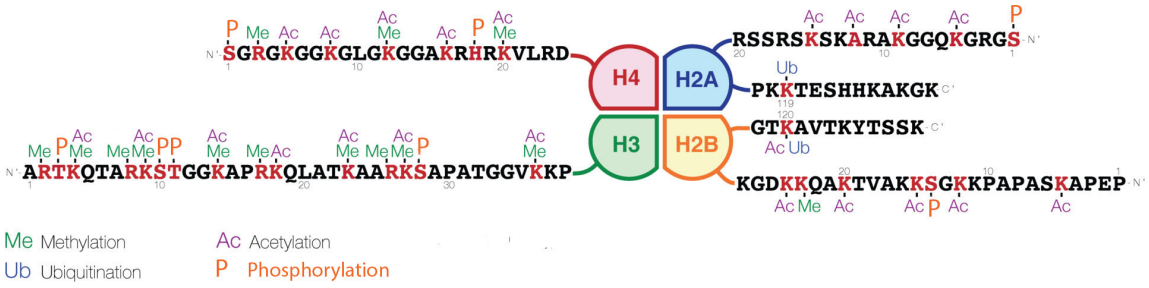

Fig. 11: Scheme of various PTMs that take place in histones.
Most of the PTM events occur in the N-terminal tails of all four histones and also in the C-terminal domain of the histone variant H2A and H2B.
Modified from [54]

There are many functions of histone phosphorylation such as regulation of chromatin compaction or regulation of transcription, however the most studied function is associated with cellular response to DNA damage, when phosphorylated histone H2AX demarcates the large chromatin domain around the site of DNA breakage. [53]

Histone H2AX is one of the histone non-allelic isoform variants that are derived from canonical histone and that differ in their primary sequence and their expression timing.[55] The H2AX histone is a member of H2A family which contains a plethora of variants with some that are found in almost all organisms, namely H2AZ and also H2AX. In general, the highest degree of diversification among this histone family is found in the C-terminus. In case of H2AX there is a special motif in the C-domain and apart from that, human H2A and H2AX differ by four amino acids in primary structure: two substitutions in the N-terminal tail, one in the L1 loop and one in the docking domain.[56]

Phosphorylation of non-canonical H2AX histone is an important modification that plays a key role in DNA damage response (DDR). This modification is one of the first events after DNA damage and occurs rapidly on serine residue near by the C-terminus of H2AX (S139) and is commonly referred to as γH2AX. The phosphorylation is dependent on action of players from the phosphatidylinositol-3-kinase (PI3K)-like group of serine/threonine kinases which includes ataxia telangiectasia mutated (ATM), ataxia telangiectasia mutated related (ATR) and DNA-dependent protein kinase (DNA-PK) (see Fig. 12 on page 28).[57] All the upstream kinases can be activated in all phases of the cell cycle and lead to a different DDR pathways.[53 58]

ATR is a kinase activated mainly in response to single stranded DNA (ssDNA) lesions and it is essential for survival of proliferating cells. Deletion of this kinase leads to early embryonic lethality in mouse, which refers to the fact that the ATR kinase is required to protect cells from replication stress and maintain the genome stability. [59] ATR kinase form a stable complex with ATR interacting protein (ATRIP) which is essential for the ATR activation. ATRIP interacts with replication protein A (RPA) that coats ssDNA chain in the site of DNA lesion and promotes the localization of ATR to the site of DNA damage or to the site of replication stress.[60] The full activation of ATR signalling requires not only ATR itself and DNA damage sensors, but also proteins function as signal transducers and effectors in the DDR network. There have been identified a lot of proteins that contribute and affect the ATR pathway and many of them are about to be discovered. It is important to mention that the ATR pathway may also lead to phosphorylation of checkpoint 1 (Ser317) that leads to cell cycle arrest. Beside the cell cycle arrest, ATR pathway activates factors involved in DNA damage repair or in apoptotic pathway.[61]

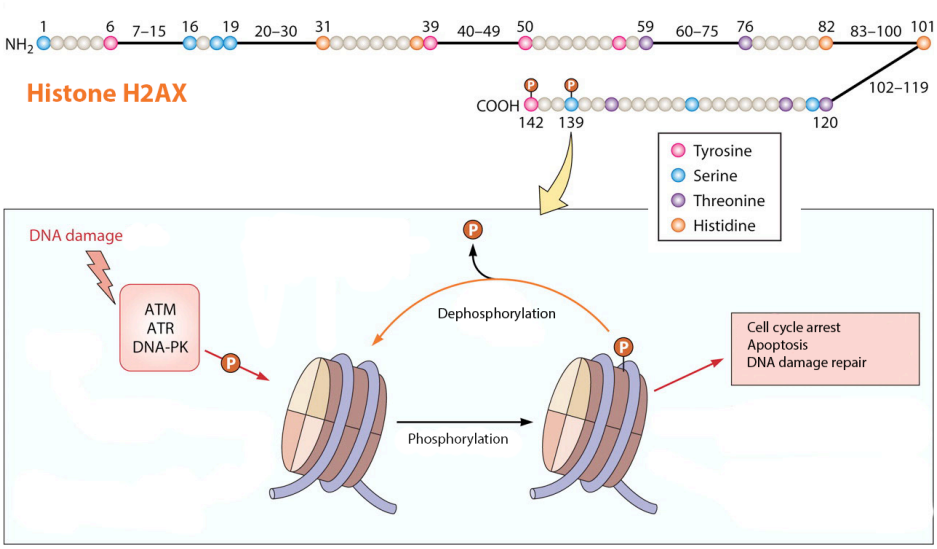

Fig. 12: The histone H2AX variant and its phosphorylation as an answer to DNA damage.
After DNA damage the ATM, ATR or DNA-PK is activated to signal the DNA lesion. This DDR leads to cell cycle arrest, apoptosis or DNA damage repair.
Modified from [62]

ATM kinase was named after the autosomal recessive disorder ataxia telangiectasia that is caused by mutation in the ATM gene. The clinical manifestation of the disease includes immune defects, cerebellar degeneration, genome instability and malignity. ATM kinase is activated mainly after double stranded DNA (dsDNA) breaks and the activation leads to phosphorylation of number of downstream substrates such as checkpoint kinase 2 (Chk2), p53 protein, KAP1 protein and Brca1.[63] In non-stress condition, ATM forms a multimer in the cell nucleus. As the DNA lesions are recognized, ATM undergoes autophosphorylation at residue S1981 that results in dissociation of ATM multimer. Phosphorylated ATM monomer is guided to the site of dsDNA breaks by the MRN complex (Mre 11, Rad50, Nbs1) that binds to dsDNA ends. It is still not clear which signals are responsible for the ATM autophosphorylation, however it has been suggested that some of the chromatin-remodeling proteins could be involved.[61]

ATM also mediates nuclear and cytoplasmic signaling cascades that are not related to DNA repair but are instead involved in maintaining cell homeostasis.[64]

1.5 DNA repair pathways

To repair single stranded DNA lesions cells have evolved three main strategies of excision repair mechanism that are remarkably different from each other and that are also activated by different agents (see Fig. 13 on page 29).[65]

First pathway is known as base excision repair (BER), which corrects small base lesions such as alkylation, oxidation or deamination that causes little distortion of DNA helix structure. BER is initiated by DNA glycosylase, which recognises and removes the flipped out damage base, forming an abasic site (AP-site). This site is a target for a concerted AP endonuclease that cleaves AP site, resulting in single stranded DNA breaks. Further processing can take place by "short-patch" BER in which single nucleotide gap is generated or by "long-patch" BER in which a gap of 2-10 nucleotides is generated and filled. Both strategies include different DNA polymerase and DNA ligase that repair the ssDNA breaks. The undamaged strand acts as a template for DNA polymerase that restores the original sequence and the remaining break is then sealed by DNA ligase.[66 67]

The major pathway, that removes bulky DNA lesions, which induce considerable distortion of DNA helix structure that is known as nucleotide excision repair (NER). Most of these DNA adducts are caused by UV light that creates cyclobutane pyrimidine dimers, pyrimidine-pyrimido photoproducts, or by numerous chemical compounds. Eukaryotic NER consists of two distinct subpathways for DNA damage recognition: global genome NER, which operates through the whole genome (independent on transcription) and transcription-coupled NER, which removes lesions specifically from transcriptionally active regions. The following excision of the section of DNA in which an error occurred seems to proceed through the same pathway. After removing that section from one strand of DNA, the second strand acts as a template and DNA polymerase can synthesize a complementary sequence. The final step is performed by DNA ligase that forms double strand DNA. This complex process relies on the products of more than 30 genes.[68 69]

Another pathway is specific for base-base mismatches generated during DNA replication, when errors created in replication escape the proofreading function of DNA polymerase, and also during recombination. This pathway is called mismatch repair (MMR) and plays a key role in maintaining genomic stability.[70 71]

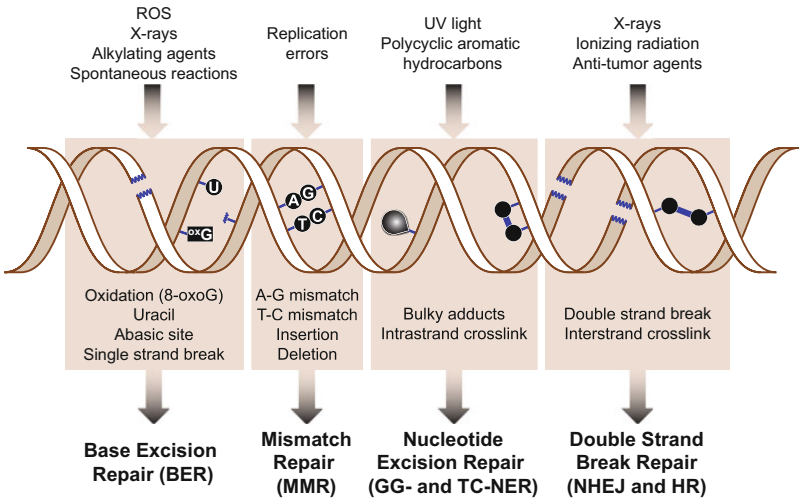

Fig. 13: Various sources of DNA damage cause different types of DNA lesions that activate different repair mechanisms.
Taken from [72]

The most dangerous type of DNA damage are dsDNA breaks. The presence of unrepaired dsDNA breaks poses serious threats to genetic stability and integrity. For instance, single unrepaired dsDNA break triggers DDR pathway that leads to cell cycle arrest and, in some cases, even to cell apoptosis. In addition, inaccurate repair dsDNA breaks can also lead to loss of genetic information or chromosomal aberration. To avoid such an event, cells have elaborated two main mechanisms by which dsDNA breaks are repaired and the genome integrity is maintained.[73]

The first mechanism is known as homologous recombination (HR) and it requires a homologous DNA template to repair the DNA lesions. The occurrence of this process has been identified across all of the three domains of life and surprisingly also in viruses. Although various types of HR have been evolved in different organisms, the basic steps of this process are more or less the same.[72]

The HR begins as the ends of dsDNA breaks are resected by 5' to 3' exonuclease to produce 3' ended overhangs of single stranded DNA. Several proteins participate in the process in which the nucleoprotein filament is guided to homologous DNA sequence. Once the matching DNA sequence has been identified the strand invasion process is initiated the damaged DNA strand invades the template DNA duplex. The extension of the 3' end is carried out by DNA polymerase followed by successive ligation by DNA ligase I. In this step the four-way junctions structure (also known as a Holiday junction) is created. Next,

the recombination intermediates is resolved in one of the three possible ways, resulting in the dsDNA breaks correction.[72 74]

The second mechanism that have been evolved to repair dsDNA breaks is non-homologous end joining (NHEJ) and it does not require template DNA. The initial step in the process that is mediated by relatively small number of essential factors is the recognition of DNA lesions. Specific factors are recruited to the site together with a nuclease that carries out the end-processing step in which the damage nucleotides are removed and the single stranded overhangs are excised. Next, the missing nucleotides are synthesized by DNA polymerase μ and λ and the ends are joined together by ligase IV complex. Since the NHEJ is associated with the random insertions and deletions at the break site it is often regarded as an error-prone process.[72 75]

It is poorly understood how a cell determinates, whether HR or NHEJ will be used to repair dsDNA breaks. However, it is clear that the HR can proceed only in presence of a homologue and therefore it occurs mostly in S/G2 phase when the sister chromatid is nearby. Outside this phase the NHEJ is indeed the preferred option. It has been shown that in proliferating cells NHEJ repairs 75% of all dsDNA breaks while HR repairs remaining 25%.[75 76]

2 Aims and objectives

The main aim of this diploma thesis is to study the involvement of spliceosomal Prpf8 protein in ATM/ATR DNA damage response pathways. We also utilize stable cell lines carrying RP mutation in PRPF8 sequence to investigate the differences in cellular response to DNA damage.

The objectives are as follows:

1. To perform knock down (KD) of Prpf8 protein in HeLa cells and analyse DNA damage by measuring the level of γH2AX.

2. To use UV light as a source of DNA damage and observe the DNA repair potential of HeLa cells with and without the Prpf8 KD in different time points.

3. To investigate the differences in cellular response to DNA damage after UV light treatment in HeLa cell lines carrying different RP mutations in Prpf8 protein.

4. To use neocarzinostatin as a source of DNA damage and study the DNA repair potential of HeLa and RPE cells with and without the Prpf8 KD in different time points.

3 Materials and methods

3.1 Materials

3.1.1 Chemicals

1 M Tris (pH 6.8)	Sigma-Aldrich
1.5 M Tris (pH 8.8)	Sigma-Aldrich
2-mercaptoethanol	Sigma-Aldrich
absolute ethanol for analysis	Merck Millipore
APS (ammonium persulfate)	Sigma-Aldrich
DAPI (4',6-diamidino-2-phenylindole)	Southern Biotech
dH2O	
DMSO	Sigma-Aldrich
Dry low-fat milk	Bohe Milk
DTT (dithiothreitol)	BDH Chemicals
Dulbecco's Modified Eagle Medium	Sigma-Aldrich
EGTA	Sigma-Aldrich
Fetal Bovine Serum	Biochrom
Fluoromount-G	Southern Biotech
Glycerol	Lechner
Glycine	Sigma-Aldrich
HCl	Penta
KCl	Serva
KH_2PO_4	Sigma-Aldrich
Liquid Nitrogen	
Methanol	Sigma-Aldrich
$MgCl_2$	Sigma-Aldrich
Mouse anti-GFP antibody	Abcam
Mouse anti-Prpf8 (E-5 clone) antibody	Santa Cruz
Mouse anti-Tubulin (Tu-01)	Abcam
Mouse anti-γH2AX (phospho S139) antibody	Merck Millipore
Mouse Horseradisch Peroxidase Secondary Antibody	Jackson ImmunoResearch

Na_2HPO_4	Sigma-Aldrich
NaCl	Sigma-Aldrich
NC1 siRNA	Thermo Fisher Scientific
Neocarcinostatin	Sigma-Aldrich
Nitrocellulose membrane Protran	GE Healthcare
Normal Donkey Serum	Jackson ImmunoResearch
Oligofectamin	Invitrogen
OptiMEM	Gibco
PageRulerPresteined Plus	Thermo Fisher Scientific
Penicilin/Streptomycin	Gibco
PFA	Sigma-Aldrich
Pierce BCA Protein Assay Kit	Thermo Fisher Scientific
PIPES	Sigma-Aldrich
Prpf8 siRNA	Thermo Fisher Scientific
Rabbit anti-Chk1 (phospho Ser317) antibody	Biotech
Rabbit anti-KAP1 (phospho Ser824) antibody	Abcam
SDS (dodecyl sulphate)	Sigma-Aldrich
Secondary anti-mouse DyLight 549 antibody	Jackson ImmunoResearch
Secondary anti-rabbit DyLight 549 antibody	Jackson ImmunoResearch
Sodium azide	Sigma-Aldrich
SuperSignalTM West Femto Substrate	Thermo Fisher Scientific
TEMED (tetramethylethylenediamine)	Applichem
Triton X-100	Serva
Trizma base	Sigma-Aldrich
Trypsin/EDTA	Sigma-Aldrich
Tween 20	Sigma-Aldrich

3.1.2 Instruments

BD Influx high-speed cell sorter, Becton Dickinson

Centrifuge 5417R, Eppendorf

Flow Box, Clean Air Techniek B.V.

Imager LAS-3000, Fujifilm

Incubator, SANYO

Microscope Olympus CKX41, Olympus

Mini Centrifuge MyFuge, Benchmark Scientific

Orbital Shaker OS-10, BIOSAN

pH Meter MP225, Mettler Toledo

Power Supply PowerPar Universal, BioRad

Scan^R Olympus IX81 microscopic system, Olympus

Spectrophotometr NanoDrop 2000, Thermo Scientific

Thermomixer Comfort, Eppendorf

UV CrossLinker AEX-800, Ultra-Lum

Vertical electrophoresis Mini-Protean Tetra Cell, BioRad

Vortex Genie2, Scientific Industries

Water Bath, Julabo

Weighing Scale KERN EG 420, Kern

3.2 Methods

3.2.1 Cell culture

Human cervical cancer cells (HeLa cells), retinal pigment epithelium cells (RPE cells) and stable HeLa cell lines expressing tagged Prpf8 protein variants were used in following experiments. The Prpf8-LAP stable cell lines were established in our laboratory from regular HeLa cells that were transfected with an isolated bacterial artifical chromosome (BAC) carrying the entire human PRP8 gene tagged at the protein C terminus with a localization and affinity purification (LAP) tag containing green fluorescent protein (GFP). These stable cell lines were expressing the endogenous Prpf8 protein as well as the exogenous-LAP tagged variant of Prpf8 protein. For purposes of this diploma thesis, stable

cell lines with single nucleotide mutation Prpf8-S2118F-LAP, Prpf8-Y2334N-LAP and Prpf8-WT-LAP were used. The non-mutated variant of Prpf8 protein with LAP tag was named as wild type (WT) and was used as a control in selected experiments.

Cell lines were cultured in high-glucose (4.5 g/l) Dulbecco's Modified Eagle Medium (DMEM) supplemented with 10% fetal bovine (calf) serum (FBS) and 1% Penicilin/Streptomycin at 37°C in atmosphere of 5% CO_2. Solution of trypsin (0.5%)/PBS and EDTA (0.02%)/PBS (ethylenediaminetetraacetic acid) mixed in ration 1:1 was used for passaging the cell lines in regular time interval.

1xPBS buffer:

137 mM NaCl

2.7 mM KCl

10 mM Na_2HPO_4

1.8 mM KH_2PO_4

pH was adjusted with HCl to 7.4

filled in with H_2O

3.2.2 siRNA interference

The principle of RNA interference was used to knock down the Prpf8 protein in human cells. The siRNA transfection was performed in 6-well plate (9 cm^2) or in 12-well plate (4 cm^2) depending on an experiment. In general 30-50% confluent cells were transfected with siRNA using Oligofectamine transfection reagent in presence of OptiMEM. The solutions A and B were prepared according to guidelines (see Table 1.) and mixed together. After 30 minutes of incubation at room temperature the mix (A+B) was added to cells. Cells were then incubated with the siRNA for 48 hours in incubator.

Table 1.: The composition of mix that was added to a single well in siRNA transfection

	6 well plate		12 well plate	
	A	B	A	B
20 nM siRNA	5 µl	x	2.5 µl	x
Oligofectamine	x	5 µl	x	2.5 µl
OptiMEM	80 µl	20 µl	40 µl	10 µl

The complementary siRNA (5'-CCUGUAUGCCUGACCGUUUtt-3') to Prpf8 mRNA was designed against the sequence around the STOP codon and therefore it could not affect the exogenous Prpf8-LAP protein. The exogenous Prpf8 variant was tagged with GFP in this region and could not be targeted with the siRNA. As a negaitve control, we used the commercial negative control 1 (NC1) siRNA from Ambion.

3.2.3 UV light/neocarzinostatin (NCS) treatment

UV light and NCS were used in different experiments as sources of DNA damage in cells after the siRNA treatment. In experiments where UV light was used, medium was removed from cells, the plate was then placed into UV cross-linker chamber (E=20 J/m^2, 365 nm) and cells were irradiated. After irradiation medium was added back to cells and the plate was placed back into the incubator for different period of time.

In experiments, in which NCS was used to cause DNA damage, it was important to determinate the concentration of NCS that would induce a similar level of γH2AX as the UV light. For this purpose, we prepared 60 nM stock solution of NCS/DMEM medium that was added to cells in 6-well plate (containing 1 ml of DMEM medium) in different volumes to create a concentration scale of 12 nM, 20 nM and 30 nM NCS. Using immunofluorescence technique (see below), we found that the concentration of 12 nM NCS was equivalent to the irradiation energy of 20 J/m^2 and therefore this concentration was used in further experiments.

3.2.4 Cells fixation and immunofluorescence

Immunofluorescence (IF) was used for visualization of specific proteins by fluorescence microscopy. Cells were grown on coverslips (12-well plate) that were before the use rinsed over night in 1 M HCl, washed in dH_2O and stored in 100% EtOH.

First, DMEM medium was removed from a single well and the coverslip was placed into 30 mm Petri dish. The 12-well plate with other samples was placed back into incubator for future used. Cell sample in Petri dish was washed 3x with PBS, fixed with 4% (w/v) PFA/PIPES for 10 minutes, washed 3x with PBS again and stored in PBS in 4 °C. The process described above was performed for individual coverslip from the 12-well plate in different time intervals after the 48h siRNA treatment: 0 h, 1 h, 3 h, 6 h, 12 h and

24 h after the UV light irradiation. In experiments, in which NCS was used instead of UV light, we set up different time intervals: 0 h, 0.5 h, 1 h, 2 h, 3 h, 6 h, 12 h and 24 h.

At the time when all samples were fixed, cell membranes were permeabilized by 0.5% (v/v) Triton X-100/PBS for 5 minutes, samples were washed 3x PBS and then the coverslips were moved on a drop of 5% Normal Donkey Serum in PBS for 30 minutes to block unspecific interactions. Next, the samples were washed 1x in PBS and incubated in wet chamber with primary antibody (AB) diluted in PBS for 1 hour. The dilutions of primary antibodies are mentioned in Table 2a-b. After that, samples were washed 3x with PSB and incubated for another 1 hour in wet chamber with secondary AB diluted in PBS 1:200. Finally, coverslips were washed 3x with PBS, 1x in dH_2O and mounted to microscope slides using Fluoromount G medium containing DAPI for DNA staining.

4% PFA/PIPES:

4% (w/v) paraformaldehyde (PFA)

0.1 M PIPES pH 6.9

2 mM $MgCl_2$

1 mM EGTA pH 8

filled in with H_2O

Table 2a): Primary antibodies and their dilutions used for IF

Primary AB	Dilution of primary AB
mouse anti-γH2AX (phospho Ser139)	1:200
rabbit anti-KAP1 (phospho Ser824)	1:200
rabbit anti-Chk1 (phospho Ser317)	1:200

Table 2b): Secondary antibodies and their dilutions used for IF

Secondary AB	Dilution of secondary AB
Goat anti-mouse DyLight 549	1:200
Goat anti-rabbit DyLight 549	1:200

3.2.5 Microscopy

High-content microscopy was used to measure the total intensity of phosphorylated proteins. Images were automatically acquired by Scan^R system equipped with a 60x oil

immersion objective and 1.35 numerical aperture (60x/1.35 NA). In each sample, 225 positions were scanned and each image was reconstructed from 10 Z-stacks with 300 nm Z-steps by the Analysis Scan^R software. Cell nuclei were automatically detected based on DAPI staining and proteins of our interests were identified by a specific immunostaining. Total intensity and area of DAPI and the proteins were measured.

3.2.6 Preparation of cell lysates

We used two different approaches to prepare cell lysates depending on the particular experiment.

In the first experiment, cell lysates of each cell line were obtained after the siRNA treatment and used to show the efficiency of the Prpf8 knock down. Cells in 6-well plates were washed 3x with PBS, harvest into 300 µl of 2x sample buffer A, denaturated at 95 °C for 5 min and cold down on ice.

In the second experiment, cells were washed with PBS and harvested in time point 0 h and 24 h after the 48h-long siRNA treatments, into 1 ml of PBS and deeply frozen in liquid nitrogen. They were then proceeded to protein concentration measurement (see 3.2.7).

2x sample buffer A:

4% SDS
10% 2-mercaptoethanol
20% glycerol
0.004% bromphenol blue
125 mM Tris-HCl pH 6.8
filled in with H_2O

3.2.7 Protein concentration measurement

For protein concentration measurement, we used samples that were frozen in liquid nitrogen. First, the samples were centrifuged (14.10^3 RPM, 4 °C) for 15 min, PBS was removed and the pellets were dissolved in 100 µl of 1x sample buffer B. Next, the Pierce BCA Protein Kit Assay was used to determine the protein concentration. Following the protocol, we prepared standard curve using bovine serum albumin (BSA). Next, the

working solution was prepared from reagent A (containing BCA) and B (containing $CuSO_4$) in ration 50:1. We added 200 µl of the working solution into 10 µl of each sample. Tubes were covered and incubated at 37 °C for 30 min. Finally, we measured the absorbance of newly created complex at 562 nm on NanoDrop. The concentration was calculated from obtained absorbance values for each sample according to the BSA standard curve.

4x sample buffer B:

8% SDS

40% glycerol

270 mM Tris-HCl pH 6.8

filled in with H_2O

3.2.8 SDS-PAGE and Western Blot

SDS-polyacrylamide gel electrophoresis (PAGE) was used for protein separation. First, the 8% or 12% separating and stacking gels were prepared (see Table 3 and 4 on page 41), the aperture (BioRad) was assembled and the chamber was filled with SDS running buffer. We used the 8% polyacrylamide gel for Prpf8 protein detection and in this experiment we loaded 20 µl of the sample cell lysates and Page Ruler Presteined (5 µl) was used as molecular weight marker. The 12% polyacrylamide gel was used to detect γH2AX protein in samples obtained in different time intervals (0 h and 24 h after the siRNA incubation). Protein concentration was measured and we loaded different volumes of samples to maintain the same total amount in each well. Before the samples were loaded, it was important to add 0.5 µl of bromphenol blue and DTT in ratio 1:10 to each sample and denaturate them at 95 °C for 5 minutes. Gels were run at 80 V for 40 min and at 110V for 60-90 min in presence of 1x SDS-PAGE running buffer.

Table 3.: Composition of 8% stacking and separating gel

	Stacking Gel	**Separating Gel**
40% acrylamide/N,N'-methylenebisacrylamide 37.5:1	630 µl	2.0 ml
1 M Tris-HCl, pH 6.8	630 µl	x
1.5 M Tris-HCl, pH 8.8	x	2.5 ml

10% SDS	25 µl	100 µl
dH_2O	3.65 ml	5.3 ml
10% APS	50 µl	100 µl
TEMED	5 µl	6 µl

Table 4.: Composition of 12% stacking and separating gel

	Stacking Gel	**Separating Gel**
40% acrylamide/N,N'-methylenebisacrylamide 37.5:1	630 µl	3 ml
1 M Tris-HCl, pH 6.8	630 µl	x
1.5 M Tris-HCl, pH 8.8	x	2.5 ml
10% SDS	25 µl	50 µl
dH_2O	3.65 ml	4.35 ml
10% APS	50 µl	100 µl
TEMED	5 µl	4 µl

10x SDS-PAGE running buffer:

25 mM Tris-HCl
192 mM glycine
0.1% SDS
filled in with H_2O

After the electrophoresis was finished, the proteins were transferred onto a nitrocullulose membrane using Western Blot (WB) technique. A blotting sandwich made of sponge, 3 layers of filter papers, gel, membrane, another 3 layers of filter paper and sponge was placed to a wet WB aperture (BioRad) filled up with 1x WB transfer buffer. WB was run at 360 mA for 60 min.

1x WB transfer buffer:

25 mM Tris-HCl
192 mM glycine
20% methanol
filled in with H_2O

To detect proteins of different size, the membrane was then cut into smaller pieces, washed 1x with PBST (PBS supplemented with 0.05% Tween) on shaker and blocked with 10% (w/v) low-fat milk in PBST for 1 h. Meanwhile primary antibody was diluted in 2% low-fat milk supplemented with 0.1% sodium azide (see Table 5). The membrane was then 3x washed with PBST and incubated for 1 h with a primary antibody. Later on, the membrane was 3x washed again with PBST and incubated for 1 h with anti-mouse secondary antibody conjugated with horseradish peroxidase (HRP) diluted 1:10 000 in 2% low-fat milk. In next step, the membrane was properly washed with 3x PBST and incubated with SuperSignal West Femto Maximum Sensitivity Substrate for 2 minutes in dark. Chemiluminiscence signal was detected by LAS-3000 Imager.

Table 5.: Antibodies and their dilutions used for WB

Primary AB	Dilution
mouse anti-tubulin (Tu-01)	1:100
mouse anti-γH2AX (phospho S139)	1:1000
mouse anti-Prpf8	1:500
mouse anti-GFP	1:250

3.2.9 Data analysing

Data obtained from IF experiments were processed in Excel2016 programme. We used the Student's T-test to determinate the validity. Each experiment that was carried out at least three times. We consider the value of $p < 0.05$ as a significant value. We also calculated the standard error of the mean (SEM) to determinate the variance of sampling distribution in each experiment.

Adobe Photoshop2012, Adobe Illustrator2012, ImageJ2013 were used for processing images from microscopy and Western Blot.

4 Results

4.1 UV light and NCS activate different DDR pathways

In this diploma thesis, we use two sources of DNA damage that cause different types of DNA lesions and therefore activate different DDR pathways. We used UV light and NCS as DNA damage agents in order to understand whether the involvement of Prpf8 protein in DNA repair process is dependent on a type of DNA damage. In this experiment, we show that UV light activates ATR DDR pathway, while NCS activates ATM DDR pathway, meaning that different DNA lesions were introduced in cells. To show the difference in DDR activation after UV light irradiation and NCS treatment, we tested two antibodies that are specific to ATR and ATM DDR pathways. First, we treated HeLa cells with NCS or with UV light to induce DNA damage. The samples were stained with different combinations of antibodies (see Fig. 14 on page 44) and indirect immunofluorescence was used to analyse the cellular response to DNA damage. Antibody against pKAP1 was used for detection of ATR pathway and antibody against pChk1 was used for detection of ATM pathway, γH2AX antibody was used as a positive control for both pathways. As a negative control, we used HeLa cells without any treatment and we stained them with γH2AX antibody. The 0+2 samples (see Fig. 14 on page 44) refer to HeLa cells in which the DNA damage was induced, however only secondary antibody was used for staining to test that no unspecific interactions were present. The results showed that UV light irradiation caused increased level of pKAP1 and γH2AX in HeLa cells, however the amount of pChk1 was not influenced, suggesting that the ATR DDR pathway was specifically activated. We observed increased level pChk1 and γH2AX in HeLa cells treated with NCS, however the level of pKAP1 was not affected which suggests that the ATM DDR pathway was primary activated.

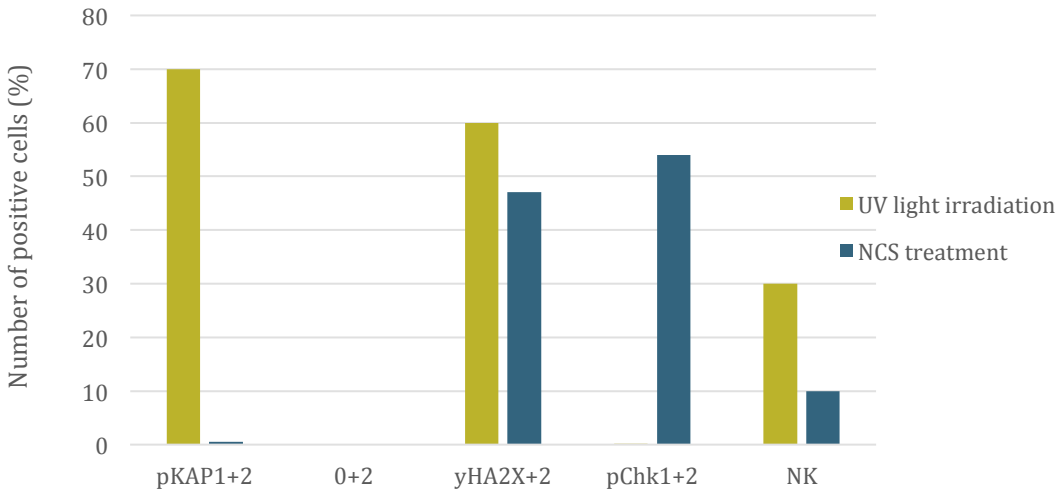

Fig. 14: An activation of different cellular events in HeLa cells after the UV light irradiation or the NCS treatment. The indirect immunofluorescence was used to measure the intensity of different antibodies.
The chart shows that UV light triggers the ATR pathway (pKAP1 antibody is increased), while the ATM pathway is triggered (pChk1 antibody is increased) by NCS treatment. The level of γH2AX in HeLa cells is almost equal after NCS/UV light treatment.

4.2 The efficiency of Prpf8 KD in different cell lines

To study the role of Prpf8 protein in cellular response to DNA damage, we knocked down the Prpf8 protein using siRNA in HeLa cells, RPE cells and HeLa-Prpf8 mutated stable cell lines. The efficiency of Prpf8 down regulation was analysed by Western Blot. We used cell lysates obtained from HeLa cells and RPE cells to show decreased expression of Prpf8 protein after the incubation with siRNA targeting Prpf8. We used NC1 siRNA as a negative control and tubulin as the loading control. The result is shown in Figure 15 on page 45. The expression of tubulin is similar in each sample, however the expression of Prpf8 protein is noticeably decreased in samples treated with Prpf8 siRNA, indicating that the Prpf8 protein was successfully down regulated.

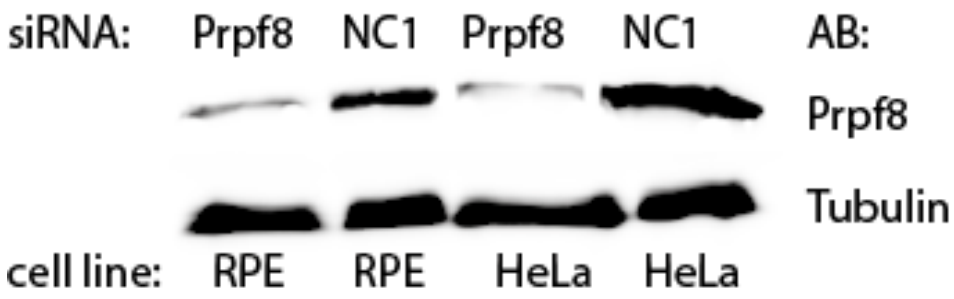

Fig. 15: Western Blot, in which expression of Prpf8 protein in HeLa and RPE cells after the Prpf8 or NC1 siRNA treatment was analysed. Tubulin was used as a loading control.
Reduced expression of Prpf8 protein was observed in HeLa cells and RPE cells after the Prpf8 siRNA treatment. NC1 siRNA treatment was used as a negative control.

Next, we used cell lysates from Prpf8-WT-LAP, Prpf8-S2118F-LAP, Prpf8-Y2334-LAP cell lines and showed decreased level of endogenous Prpf8 protein expression after the Prpf8 siRNA treatment, while expression of the exogenous LAP tagged Prpf8 proteins stayed unaffected. For this purpose, we used the anti-Prpf8 AB and also the anti-GFP AB for visualization of the exogenous-LAO tagged Prpf8 protein, which expression was not influenced by Prpf8 siRNA transfection (Fig. 16).

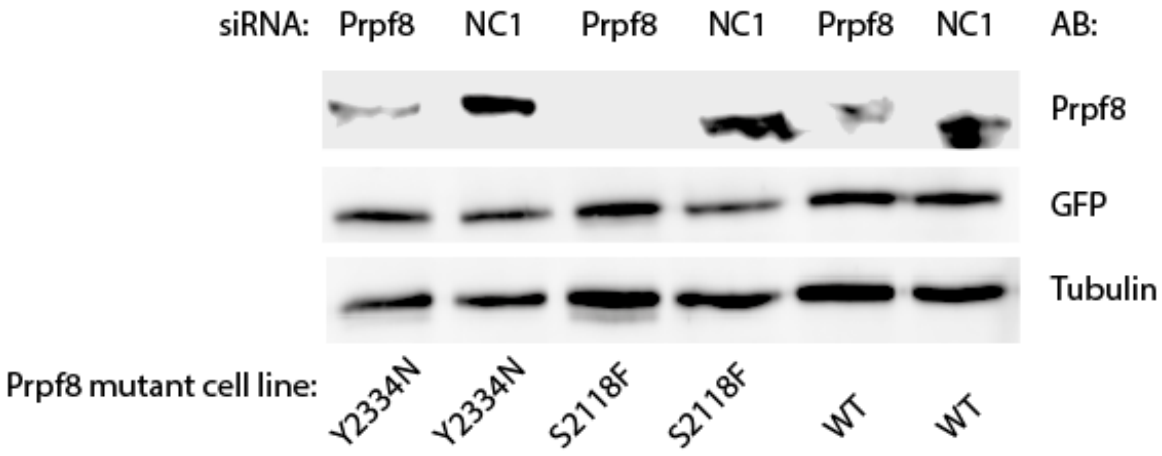

Fig. 16: The expression of Prpf8 protein after the Prpf8 or NC1 siRNA treatment detected by Western Blot in Prpf8-WT-LAP, Prpf8-S2118F-LAP and Prpf8-Y2334-LAP cell lines. Anti-GFP AB was used to visualize the unaffected expression of Prpf8-LAP protein and the anti-tubulin AB was used as a loading control.
Anti-Prpf8 AB was used for detection of the Prpf8 protein which expression was reduced after the Prpf8 siRNA transfection. Although the bands are not very sharp, the different between NC1 and Prfp8 KD samples is visible. Expression of LAP tagged Prpf8 protein correlates with loading control, suggesting that the expression of exogenous LAP-tagged Prpf8 protein was not inhibited by the Prpf8 siRNA treatment.

4.3 KD of Prpf8 does not affect the level of γH2AX

In following experiments, phosphorylation of H2AX histone variant was used as a marker for activation of DNA damage response (DDR) pathways. An overall result for each experiment described bellow is made of 3-5 biological replicates and there were approximately 3000-5000 HeLa cells detected and analysed in each sample. The relative intensity of γH2AX was normalized to the intensity of γH2AX in time point 0 h.

Before we started studying the role of Prpf8 protein in DDR pathways, it was important to prove that the KD of Prpf8 protein itself does not affect the level of phosphorylated H2AX variant (γH2AX). We treated HeLa cells with Prpf8 or NC1 siRNAs for 48h and then fixed them at different time points. We used indirect immunofluorescence method to detect the level of γH2AX in particular samples. The overall results (Fig.17) suggest that the reduced expression of Prpf8 protein does not influence the level of γH2AX in HeLa cells.

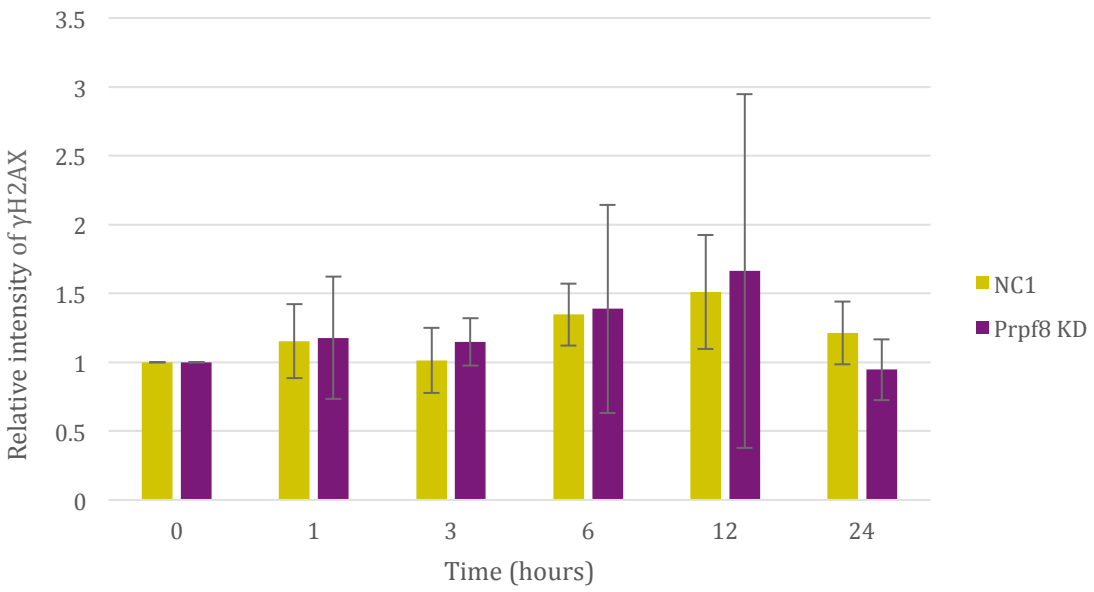

Fig. 17: Indirect immunofluorescence indicating the amount of γH2AX in various time points in HeLa cells after the Prpf8 or NC1 siRNA treatment.
The chart shows that the relative intensity of γH2AX is similar for Prpf8 KD and NC1. The level of γH2AX does not differ in various time points suggesting that the KD of Prpf8 protein does not trigger the DDR pathway. No significance was observed.

4.4 KD of Prpf8 protein influences the level of γH2AX in HeLa cells after UV light irradiation

We induced DNA damage in HeLa cells by UV light and monitored the DNA repair ability of cells by reduced signal of γH2AX. The Prpf8 KD was performed in order to study the involvement of this protein in cellular response to DNA damage. In the experiment, HeLa cells were treated with Prpf8 or NC1 siRNA for 48h and fixed in different time points after UV light irradiation (E=20 J/m^2, 365 nm). We used indirect IF and Scan^R analysis software to measure the level of γH2AX in individual samples. The results (Fig. 18) have shown that the level of γH2AX is sharply increased in first three hours after the irradiation in both samples. This trend indicates that the DDR pathway was triggered by UV light. The amount of phosphorylated H2AX histone remains approximately constant for next few hours and the biggest drop was observed after 24h. In this time point, the level of γH2AX was significantly decreased in NC1 samples, however in Prpf8 KD samples the level of γH2AX was even increased, which suggests that the DNA repair ability is negatively influenced in cells with Prpf8 knockdown. The results also indicate that the KD of Prpf8 inhibits DNA repair process.

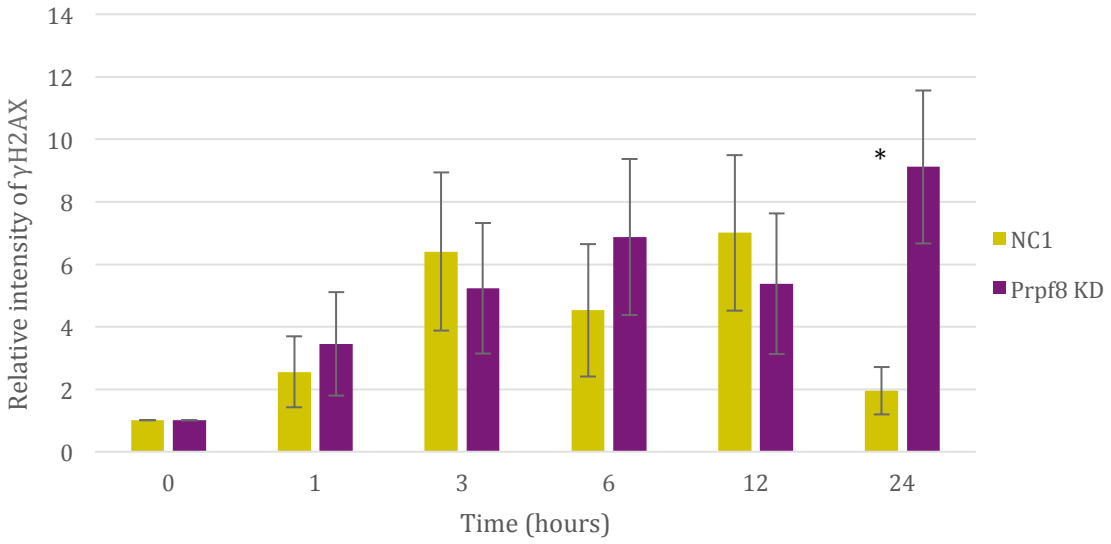

Fig. 18: The intensity of γH2AX measured by indirect immunofluorescence in different time points after the UV light irradiation in HeLa cells that were treated with Prpf8 or NC1 siRNA.
The chart shows a significant difference in time point 24 h for Prpf8 and NC1 samples, which suggests that the Prpf8 protein is important for DNA repair process.

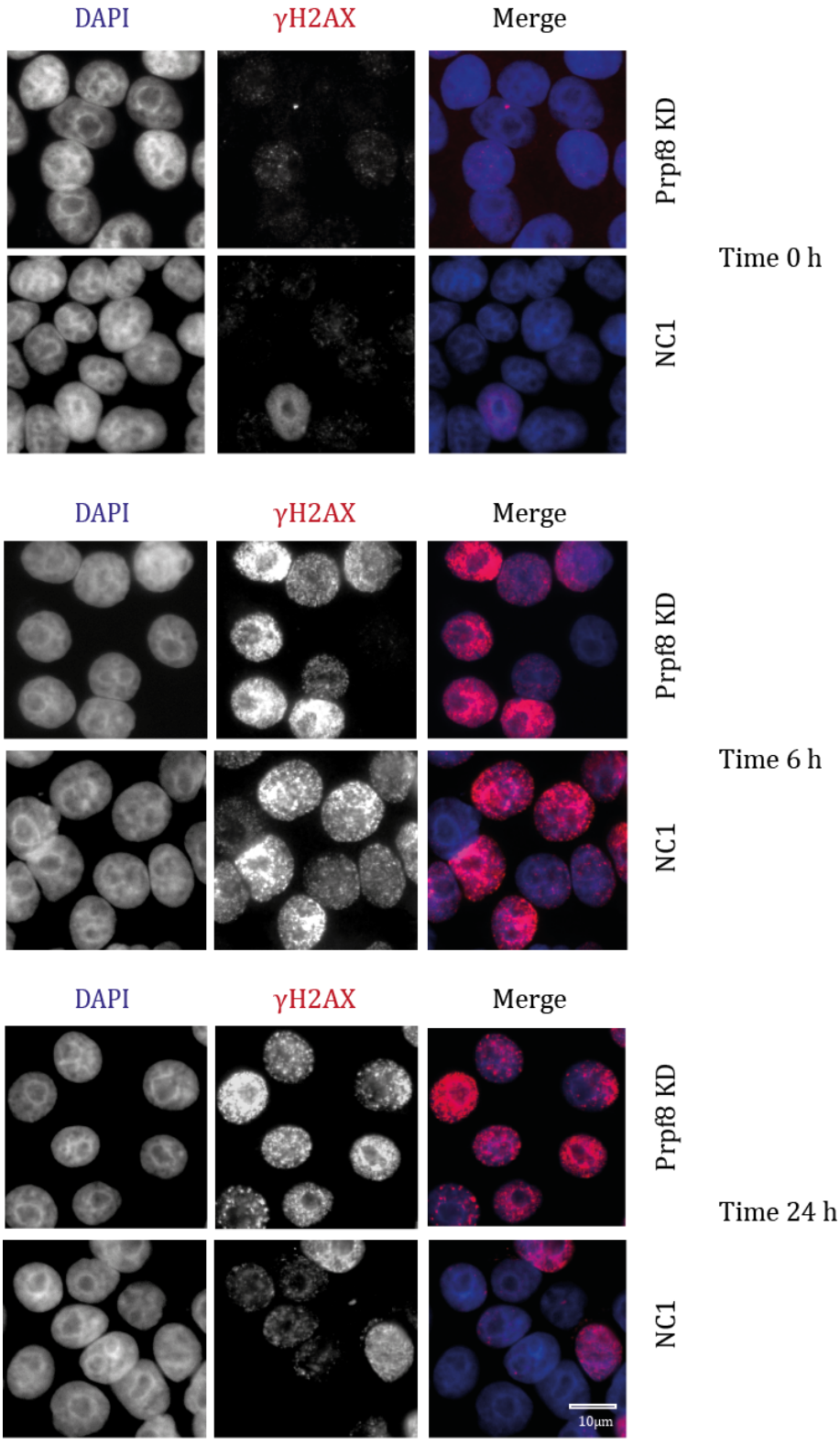

Fig. 19A-C: Intensity of γH2AX and Dapi (DNA counterstaining) measured by indirect immunofluorescence in HeLa cells that were treated with Prpf8 or NC1 siRNA. The cells were irradiated by UV light and fixed after 0 h, 6 h and 24 h after the irradiation.

These images correlate with the overall results showed in Fig. 18 (page 47). Intensity of γH2AX in time point 0 h is very low and it represents the physiological level of γH2AX in cells. In time point 6 h, the level of γH2AX is increased and it is approximately equal for NC1 and Prpf8 KD samples. The difference in

intensity of γH2AX for NC1 and Prpf8 KD cells is clear after 24 h after UV irradiation. In this time point, the NC1 cells show a decreased level of phosphorylated H2AX, however the intensity of γH2AX for Prpf8 KD cells is even increased. The merge shows γH2AX in red and DAPI in blue.

Selected images obtained from fluorescence microscopy demonstrate the differences in phosphorylation of H2AX histone variant in various time points for the NC1 and the Prpf8 KD samples (see Fig. 19 A-C on page 48). In figure 19A, the cells were fixed immediately after the UV light irradiation (0 h) and we observed only a physiological level of γH2AX which correlated with the level of histone H2AX phosphorylation in cells that were not treated with UV light. In figure 19B, the signal of γH2AX is noticeably increased in nuclei (marked by DAPI staining) in both samples. The high intensity of γH2AX signal indicates that the cellular response to DNA damage has been triggered. The difference in γH2AX intensity for NC1 sample and Prpf8 KD sample is visible in time point 24 h, indicating the lower DNA repair ability for Prpf8 KD cells (Fig. 19C).

To verify the different level of γH2AX for NC1 and Prpf8 KD samples in time point 24 h after the UV light irradiation we used Western Blot technique. HeLa cells were incubated with Prpf8 or NC1 siRNA for 48 h and then irradiated by UV light (E=20 J/m^2, 365 nm). Cell lysates were obtained in time point 0 h and 24 h after the irradiation. To ensure the equal loading of proteins on the gel, we measured protein concentration using BCA assay. After the WB, we used performed immunostaining of the membrane to detect the γH2AX protein a tubulin.

The result (Fig. 21 on page 50) showed a very low level of γH2AX for NC1 and Prpf8 KD samples that were fixed immediately after UV light irradiation. Increased level of γH2AX was observed after 24 h in both samples, however the intensity of band for Prpf8 protein was higher comparing to NC1 sample. This result indicates slightly different trend comparing to the result obtained from IF (Fig. 18 on page 47) that showed only basal level of γH2AX in time point 24 h for NC1.

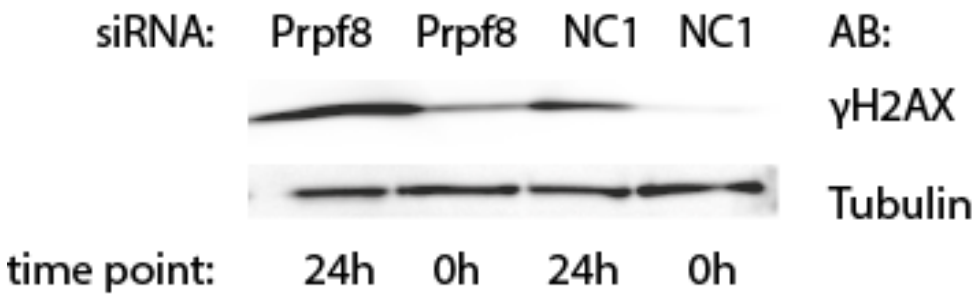

Fig. 20: Western Blot, in which the amount of γH2AX in HeLa cells treated with Prpf8 or NC1 siRNA was measured, in time points 0 h and 24 h after the UV light irradiation. Tubulin was used as a loading control.
The figure shows different intensity of γH2AX bands for Prpf8f and NC1 samples fixed after 0 h or 24 h after the UV light irradiation. Samples obtained in time 0h represent negative control that is characterized by a low level of γH2AX. After 24 h, we observed γH2AX signal in both samples, however the intensity of γH2AX was higher in Prpf8 sample.

4.5 RP mutants show different response to DNA damage

Next, we studied roles of Prpf8 mutants that are linked to RP in DNA damage response. We used stable cell lines carrying RP mutation in Prpf8-LAP tagged protein that were established in our laboratory by BCA recombineering assay and we analysed their responses to DNA damage caused by UV light irradiation. We knock down the endogenous Prpf8 protein in the Prpf8-S2118F-LAP cell line, Prpf8-Y2334N-LAP cell line and Prpf8-WT-LAP cell line, meaning that only the LAP-tagged Prpf8 protein was expressed (Fig. 16 on page 45) and we investigated the ability of individual cell lines to repair the DNA lesions. The results (Fig. 21 on page 51) have shown the similar trend for the Y2334N and WT samples in which the intensity of γH2AX was increasing in first hours and the peak was reached after 3 hours after the UV light irradiation. During next hours the level of γH2AX was decreasing which suggest that the Y2334N and WT mutants were able to repair the DNA damage. This result is similar to the trend that was observed for NC1 samples, Fig. 18 on page 47. Different trend was observed for the S2118F mutant that showed an increasing level of γH2AX in first hours, however the peak was reached in time point 24 hours after the UV light irradiation which indicates that the S2118F variant of Prpf8 protein could not rescue down regulation of endogenous Prpf8 protein and therefore the DNA damage was not repaired.

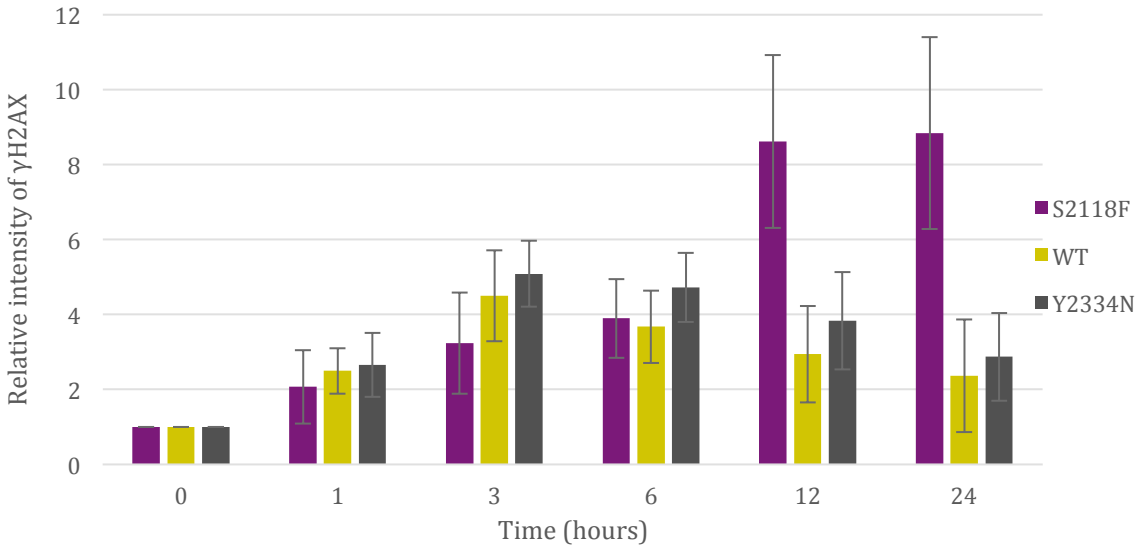

Fig. 21: Indirect immunofluorescence, in which the intensity of γH2AX was measured in different time points after the UV light irradiation in Prpf8-WT-LAP, Prpf8-S2118N-LAP and Prpf8-Y2333N-LAP cell lines.
The chart shows different responses to DNA damage in various cell lines carrying RP mutations. Unfortunately, the results were not significant, although the trend indicates that S118F mutants could not rescue the Prpf8 KD in contrast to the Y2334N mutant.

The level of γH2AX in various samples is demonstrated on representative microscopic images in Fig. 22A-C on page 52. The amount of phosphorylated H2AX histone is very low for each cell line in time point 0 h (Fig. 22A) after the UV light irradiation and it corresponds with the negative control. The level of γH2AX is clearly increased in all RP mutants (Fig. 22B) in time point 6 h after the UV light irradiation, which indicates that the DNA damage cellular response was activated. The difference is obvious in time 24 h (Fig. 22C) in which the WT and Y2335N samples showed reduced intensity of γH2AX, suggesting that the DNA damage was repaired. A different trend was observed in S2118F mutant, in which the level of γH2AX was not decreased meaning that the DNA damage was not repaired properly.

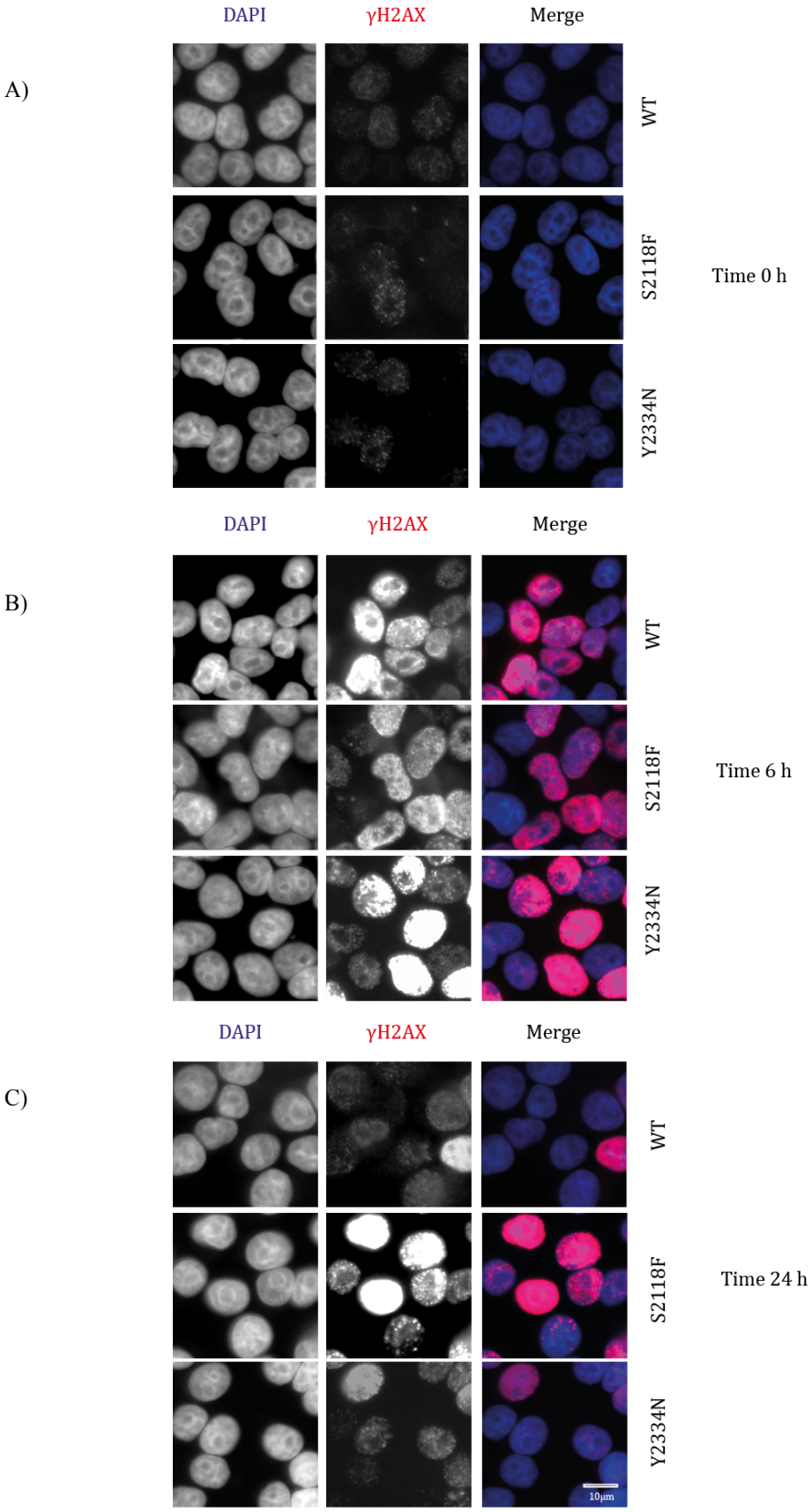

Fig. 22A-C: Various amounts of γH2AX after the UV light irradiation in the Prpf8-S2118F-LAP, Prpf8-Y2334N-LAP and Prpf8-WT-LAP cell lines measured by indirect immunofluorescence after 0 h, 6 h and 24 h after the irradiation.

We used various stable cell lines carrying RP mutations to study the cellular response to DNA damage. In representative images, the signal of γH2AX was measured in cell lines in time point 0 h, 6 h and 24 h after the UV light irradiation. The level of γH2AX was low for cells that were fixed immediately after the UV light treatment, which corresponds with previous results (Fig.19A-C, page 48) and suggests that the DDR pathway has not been activate yet. The next selected images represent samples fixed after 6 hours after the irradiation, and the increased level of γH2AX is visible for each cell line. The drop in intensity of γH2AX is clear in time 24 h for the Y2334N and WT cells, however the intensity of γH2AX reminds constant for the S2118F mutant.

To verify the results (Fig. 21 on page 51), the same experiment using Western Blot as described above was performed. The level of γH2AX was measured in cell lines carrying RP mutations in time 0 h and 24 h after the UV light treatment. The results (Fig. 24 on page 53) showed a similar phenotype for WT and Y2334N samples, in which the amount of phosphorylated H2AX histone was low in time 0 h and during the time it was increased. Different trend was observed in S2118F mutant, which showed a noticeably higher level of γH2AX in time 0 h, comparing to other samples, although the signal for tubulin was also stronger. After 24 h from the UV light treatment, the S2118F mutant showed even more increased level of phosphorylated H2AX histone.

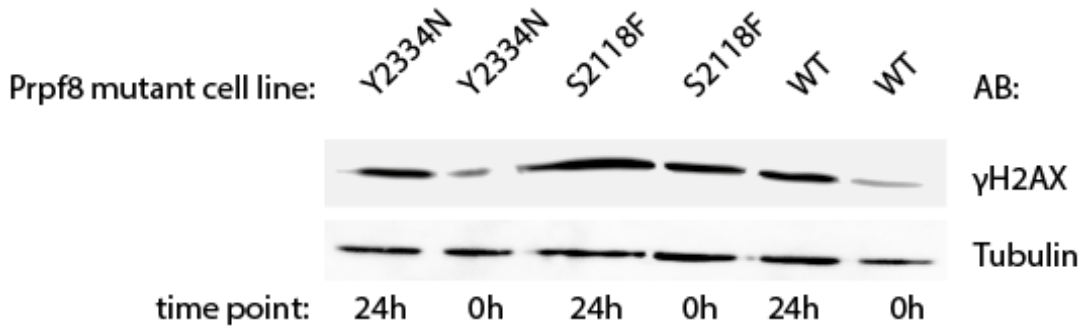

Fig. 24: Western Blot, in which the amount of γH2AX in Prpf8-S2118F-LAP, Prpf8-Y2334N-LAP and Prpf8-WT-LAP cell lines irradiated with UV light, was analysed. The cells were harvest in time point 0 h and 24 h after the irradiation and tubulin was used as a loading control.
The figure shows differences in γH2AX levels for individual samples. While the trend observed in WT and Y2334N samples was similar, the S2118F mutant showed increased level of γH2AX in both time points, compering to other samples.

4.6 Down regulation of Prpf8 protein does not affect the level of γH2AX after the NCS treatment

In the second part of the diploma thesis, we used neocarzinostatin (NCS) as a source of DNA damage that causes specifically dsDNA breaks which trigger the activation of ATM pathway in order to repair the DNA damage. We observed the DNA repair potential of HeLa and RPE cells after the NCS treatment and we also investigated the involvement of Prpf8 protein this process.

4.6.1 Determination of NCS concentration in HeLa cells

First, we determined the concentration of NCS that induced the similar level of γH2AX in HeLa cells as the UV light irradiation. For this purpose, the cells were treated with various concentrations of NCS and fixed in different time points. Cells without NCS treatment were used as a negative control and the final relative intensity of γH2AX of each sample was normalized to the intensity of γH2AX in untreated cells. The amount of phosphorylated H2AX histone as a response to different NCS treatment in time is showed in Figure 25. We compared the obtained values with results we observed after the UV light irradiation and chose the 12nM concentration of NCS for further experiments.

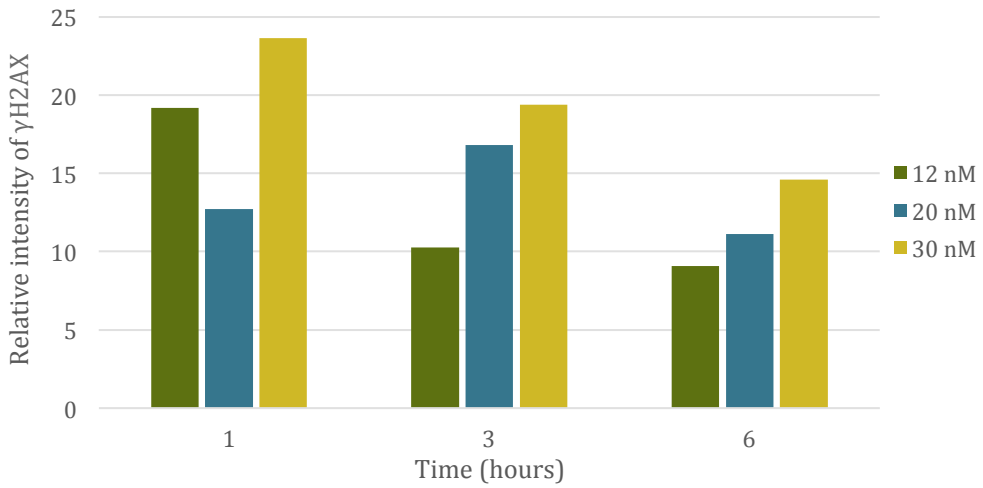

Fig. 25: Indirect immunofluorescence measuring the level of γH2AX in HeLa cells that were treated with different concentrations of NCS and fixed in different time points after the NCS treatment.
The samples were incubated with various concentrations of NCS for 1 h, 3 h and 6 h in purpose to find the right concentration for further experiments.

4.6.2 The cellular response to DNA damage caused by NCS

First, we treated the Prpf8 KD HeLa cells and the NC1 treated HeLa cells with 12nM NCS to induce DNA lesions. The samples were fixed in time points 0.5 h, 1 h, 2 h, 3 h, 6 h, 12 h and 24 h and the intensity of γH2AX was measured. However the results showed variations in intensity of γH2AX for Prpf8 KD and NC1, the dissimilarities are not significantly different in any sample (Fig. 26)

Interestingly, the amount of phosphorylated H2AX histone is almost identical for Prpf8 KD and NC1 samples in time point 24 h. This suggests that the cells were able to repair the DNA lesions caused by NCS despite the Prpf8 protein was down regulated

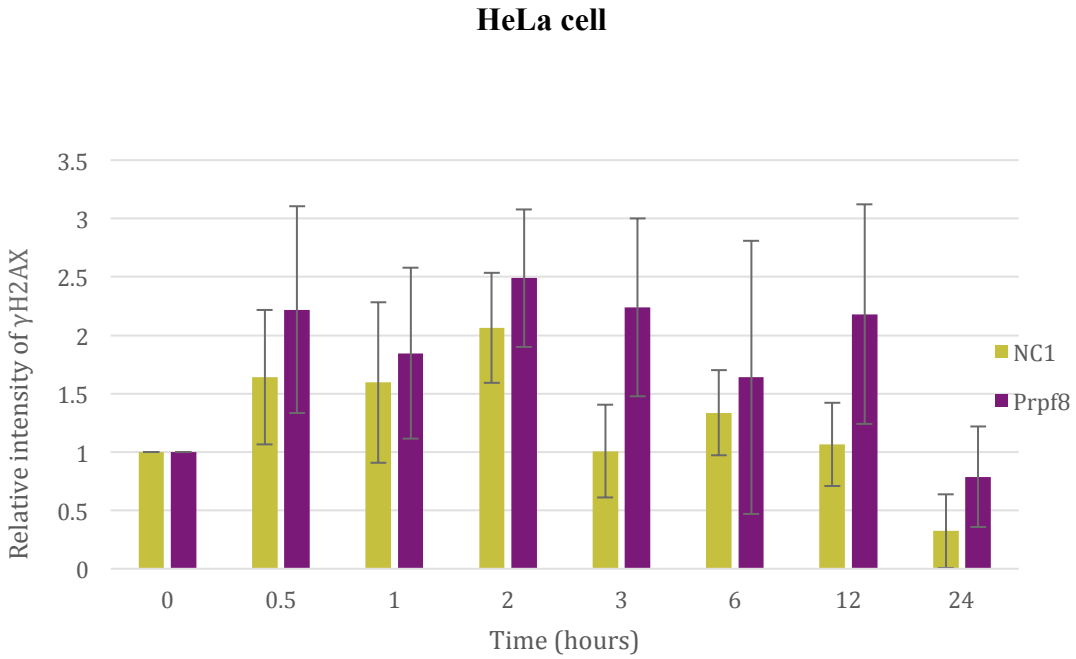

The Fig. 26: The amount of γH2AX for NC1 and Prpf8 KD samples obtained from HeLa cells after the NCS treatment measured by indirect immunofluorescence in various time points after the treatment. Samples were fixed in different time points after the NCS treatment and the level of γH2AX was measured to investigate the cellular response to DNA damage. Surprisingly, the amount of γH2AX is similar for NC1 and Prpf8 KD samples after 24 hours of incubation with NCS, suggesting that the Prpf8 protein is not involved in DDR pathway, which is activated after the NCS treatment.

Distribution of a γH2AX signal in Prpf8 KD and NC1 samples after 2 hours of incubation with NCS is compared to negative control in selected microscopic images in Fig. 27 (on page 56). The signal of γH2AX, that was detected in HeLa cells after NCS treatment showed different shape and distribution comparing to the signal of γH2AX that

was observed in HeLa cells after UV light irradiation (Fig 19A-C on page 48). That suggests that different type of DNA damage was induced after NCS treatment.

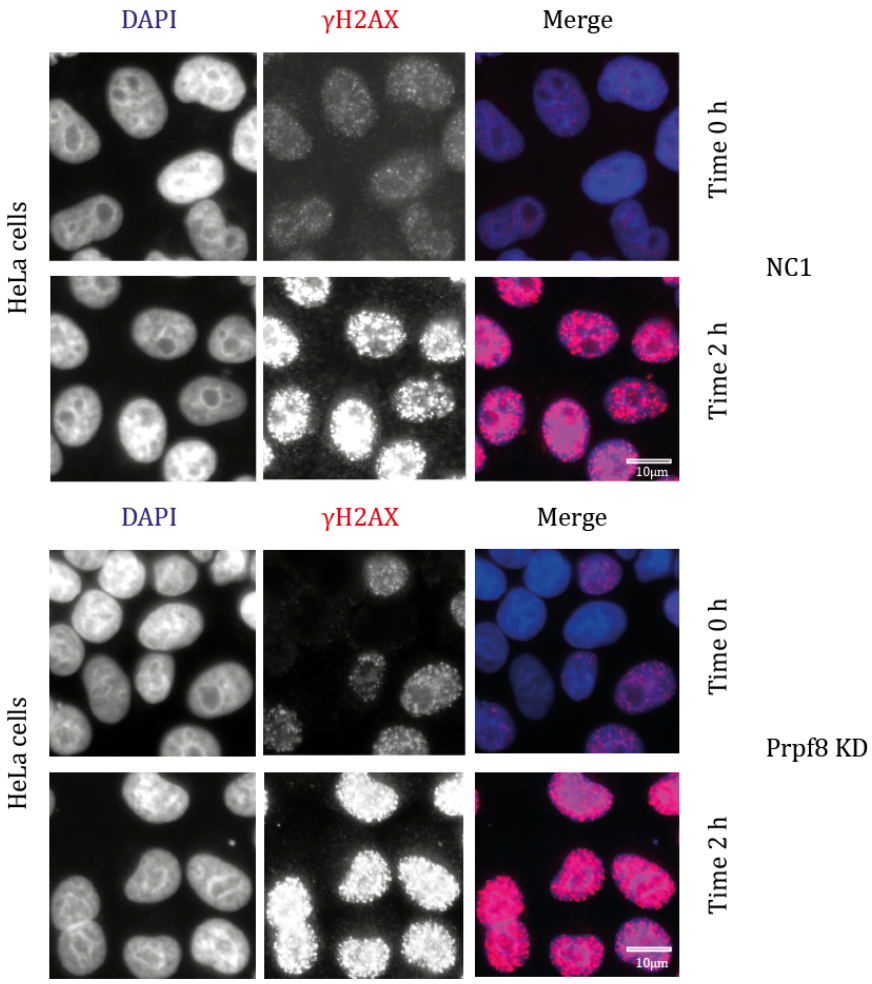

Fig. 27: Intensity of γH2AX and Dapi (DNA counterstaining) measured by indirect immunofluorescence in HeLa cells that were treated with Prpf8 or NC1 siRNA. The cells were incubated with NCS for 0 h or 2 h.
Similar amount of phosphorylated H2AX histone in time point 2 h after NCS treatment was observed for NC1 and Prpf8 KD samples. We detected formation of nuclei foci of phosphorylated H2AX histones as a response to DNA lesions induced by NCS treatment.

Additionally, we performed the same experiment with RPE cells to compare the cellular response to DNA damage in various cell types. The intensity of γH2AX in different time points after NCS treatment for NC1 and Prpf8 treated RPE cells is showed in Fig. 28 (on page 57). We observed a similar response in RPE cells as in HeLa cells to NCS treatment.

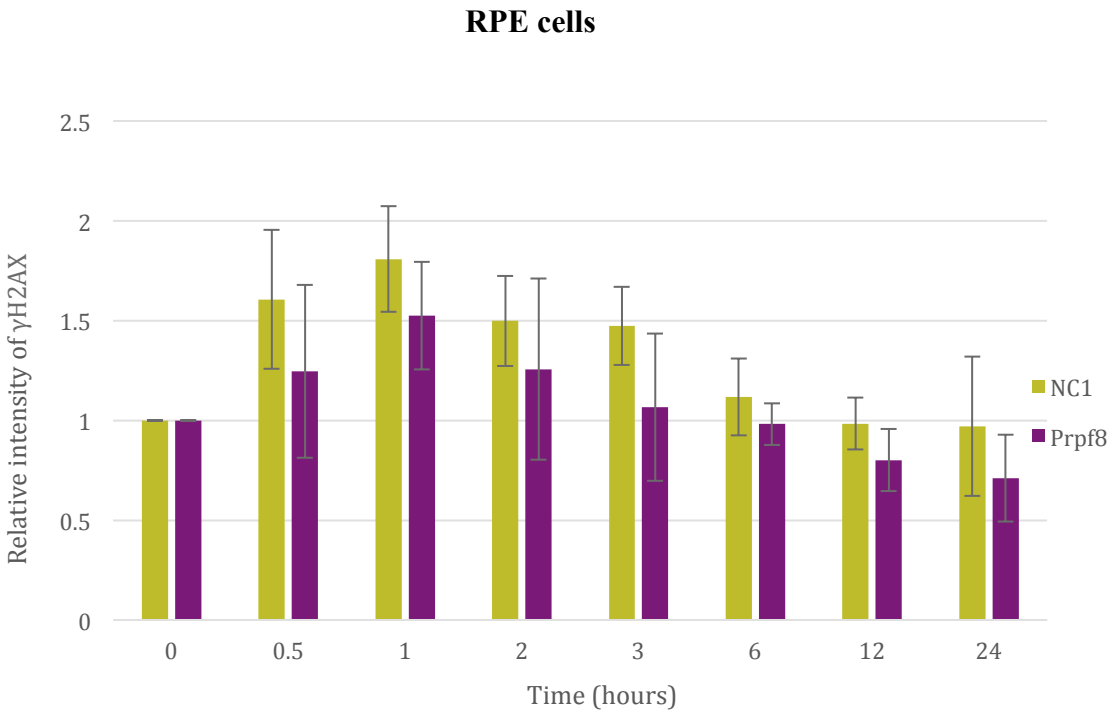

Fig. 28: The amount of γH2AX in NC1 and Prpf8 KD samples obtained from RPE cells after the NCS treatment measured by indirect immunofluorescence in various time points after the treatment.
The result did not show any significant differences for NC1 and Prpf8 KD samples in any time point, suggesting that the Prpf8 protein is not involved in DDR pathway that is activated after the NCS treatment.

The microscopy images of RPE cells fixed in time 0 h and 2 h after the NCS treatment for NC1 and Prpf8 KD samples show the low increase in intensity of γH2AX (Fig. 29 on page 58). The overall amount of RPE cells that were observed by IF was lower comparing to HeLa cells, which may refer to slower cell growth and cell division of RPE cells. The formation of phosphorylated H2AX histones nuclear foci was detected in RPE cells and it corresponds with the observation in HeLa cells.

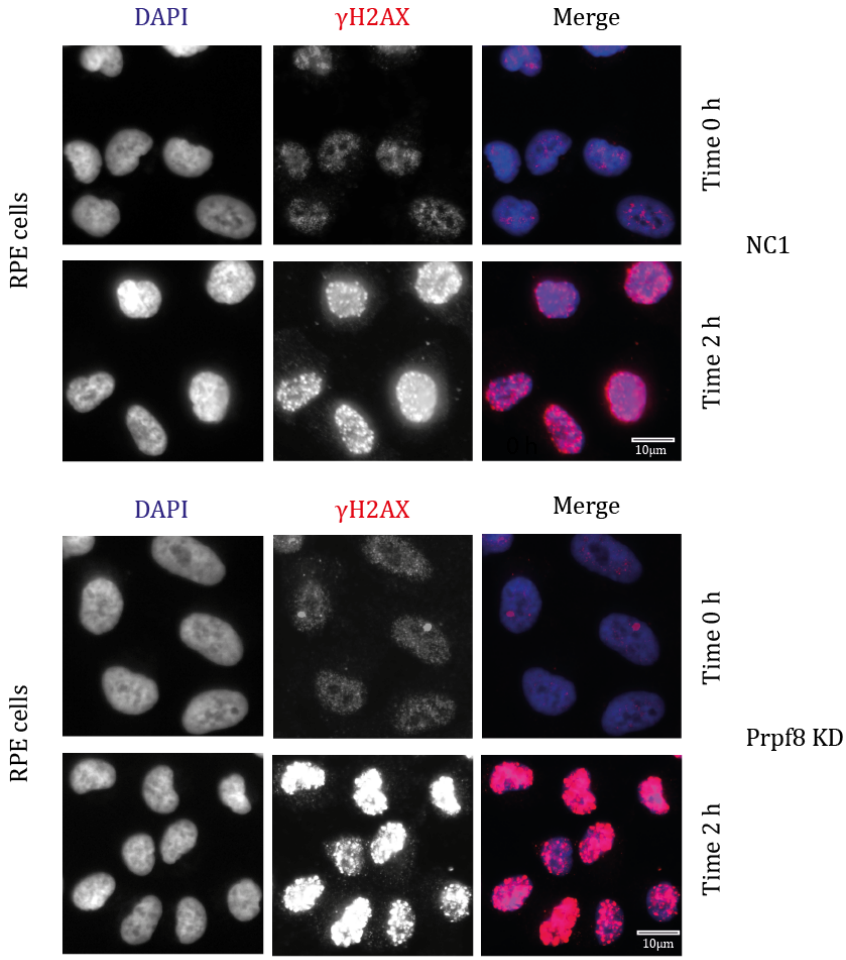

Fig. 29: Intensity of γH2AX and Dapi (DNA counterstaining) measured by indirect immunofluorescence in RPE cells that were treated with Prpf8 or NC1 siRNA. The cells were incubated with NCS for 0 h or 2 h.
Similar amount of phosphorylated H2AX histone in time point 2 h after NCS treatment was observed for NC1 and Prpf8 KD samples. We detected formation of nuclei foci of phosphorylated H2AX histones as a response to DNA lesions induced by NCS treatment.

5 Discussion

Splicing of nuclear pre-mRNA is an essential process by which introns are removed from a pre-mRNA and exons are joined together to produce a mature mRNA. This process is catalysed by spliceosome, a large macromolecular complex that contains five snRNPs and more than 150 associated proteins.[3] In this thesis, we focused on Prpf8 protein that is a major component of the catalytic U5 snRNP and mutations in this protein have been connected to disease known as retinitis pigmentosa. RP is a hereditary retinal disorder causing gradual degeneration of photoreceptor and retina cells which leads to decreased night vision, reduction of field vision and in advanced stadium, it could cause total blindness.[35 39]

Here, we tested our hypothesis that the Prpf8 protein is involved in cellular response to DNA damage. We also tested whether exogenously expressed RP mutated Prpf8 proteins are capable to rescue the effect of KD of endogenous Prpf8 protein to the same level as WT.

We used two sources of DNA damage that induce different types of DNA lesions, which activate different DDR pathways. First, we used UV light, that is one of the most common cause of DNA lesions and especially of the cyclobutane pyrimidine dimers and the pyrimidine-pyrimido photo products.[77] In parallel, we used neocarzinostatin which is a drug composed of two parts, a labile chromophore that is tightly bound to a protein which protects the unstable potential DNA damaging agent.[78] In contrast to UV light, that causes various types of DNA lesions which are mainly sensed by the ATR DDR pathway[79], NCS triggers exclusively the ATM DDR pathway that repairs dsDNA breaks that are specific products of NCS treatment.[80] We chose two different cellular processes that are specifically triggered by the ATR or ATM pathway and we tested their presence by specific antibodies after the UV light irradiation or after the NCS treatment to present evidence, that these agents evoke activation of different DDR pathways. Since the ATR kinase rapidly phosphorylates the Chk1 in response to DNA damage, we used the Chk1 (phosphoSer317) antibody to detect activation of the ATR pathway.[81] Currently, the KAP1 (phosphoSer824) antibody was used to detect the activation of ATM pathway.[82] We also used the γH2AX antibody to show that the phosphorylation of H2AX histone variant occurs equally after the ATR and the ATM pathway activation (Fig. 14 on page 44).

To investigate the involvement of Prpf8 protein in DNA damage response, we performed knockdown of this protein in HeLa cells (Fig. 15 on page 45), which was shown not to affect the level of γH2AX (Fig. 17 on page 46), and we irradiated the cells with UV light. The results (Fig. 18 on page 47) showed almost equally increasing level of γH2AX in first 12 hours after UV light irradiation for NC1 and Prpf8 KD samples, strongly suggesting that the UV light irradiation induced DNA damage. Interestingly, we observed a significant difference in level of γH2AX for NC1 and Prpf8 treated cells. The NC1 samples showed reduced level of γH2AX after 24 hours after UV light irradiation, which suggest that the cells were able to repair the DNA damage. In contrast, high level of γH2AX was observed after 24 hours after UV light irradiation in Prpf8 KD samples that indicates problems with DNA damage repair. There have been many studies, which showed that proteins involved in pre-mRNA splicing are modified in response to DNA damage. These post-translation modifications of splicing factors regulate their localization, stability and also promote expression of specific proteins involved in DDR via AS. There is also evidence that Prpf8 protein is phosphorylated in response to DNA damage caused by ionizing radiation, which indicates its involvement in DDR. Our finding that down regulation of Prpf8 protein leads to DNA repair disability correlates with that evidence, however the mechanism remains unclear.[83] We did not find any conclusively explanation why the level of γH2AX in Prpf8 KD samples is increasing even after 12 hours after UV light treatment, although it is possible that the process of apoptosis was activated when the DNA damage was not repaired. This theory would also explain why we detected less cells in time point 24 hours in Prpf8 KD samples comparing to the NC1 samples. It is worth it to mention that the standard error of mean for each sample was relatively high which may be due to the unsynchronized cell population that was used and which response to DNA damage may differ. The process of UV light irradiation itself could also cause minor deviations in an overall result, however it should be mentioned that the difference between control and Prpf8 KD was significant which supports our conclusion that Prpf8 protein plays an important role in DDR.

To study whether the RP mutations in Prpf8 protein affect Prrpf8 function in DDR, we set the same experiment for stable HeLa cell lines carrying RP mutation in Prpf8-LAP tagged protein. We verified the efficiency of endogenous Prpf8 protein KD by WB and showed that siRNA used to reduce endogenous Prpf8 protein does not target the LAP-tagged Prpf8 proteins. The results (Fig. 16 on page 45) showed a decreased level of

endogenous Prpf8 protein in samples treated with Prpf8 siRNA, however the amount of Prpf8-LAP protein was not affected. The blurred appearance of obtained bands may be due to the fact that Prpf8 is a large protein of 220 kDa and it is difficult to resolve it by SDS PAGE electrophoresis and transfer to a nitrocellulose membrane. Finally, the results (Fig. 21 on page 51) showed that the Prpf8-Y2334N mutant completely rescued down regulation of endogenous Prpf8 protein and exhibited the similar phenotype as the Prpf8-WT. This finding corresponds with our previous results which showed that the Y2334N mutant was able to partly complement the endogenous Prpf8 protein in pre-mRNA splicing process and that this mutant did not affect formation of the U5 snRNP.[18] This trend was identified for Prpf8-S2118F mutant that showed no reduction of γH2AX after UV light irradiation. Unfortunately, the standard error of mean was high for this experiment and therefore the results were not significant, which unable us to make a conclusion from this experiment. In future, we would like to optimise this experiment and confirm our hypothesis that the S2118F mutant does not complement the endogenous Prpf8 in DDR as it was shown for pre-mRNA splicing. [19]

To confirm results obtained from IF, we decided to perform WB and analyse the differences in level of γH2AX after 24 hours after the UV light irradiation for Prpf8 KD (Fig. 20 on page 50) and RT mutants (Fig. 24 on page 53) samples. Unfortunately, the results obtained from WB did not fully correspond with the IF results, which may be due to lower sensitivity of WB comparing to IF. Another explanation may be that the Scan^R analysis used in IF experiment, was adjusted to only analyse cells of particular shape and size to avoid analysing of apoptotic or mechanically damaged cells. In contrast, generally the WB analysis took in count all cells presented in cell lysates, which could also include apoptotic or stressed cells that have naturally increased level of γH2AX.[84]

To investigate whether the involvement of Prpf8 protein in DDR is dependent on a type of DNA damage, we used NCS treatment instead of the UV light irradiation to observe the cellular response to the DNA damage agent that causes specifically dsDNA breaks. Here, we used HeLa cells and also human RPE cells in order to compare the DNA damage response in two different cell lines. We also set slightly different time points for cell fixation after the NCS treatment, because the NCS induces DNA lesions earlier comparing to the UV light irradiation. However we used IF to determinate the concentration of NCS (Fig. 25 on page 54) that induce a similar level of γH2AX as the UV light irradiation (E= 20 J/m^2), the overall results showed in general a lower intensity of

γH2AX in HeLa and RPE cells after NCS treatment (Fig. 26 and 27 on page 55-56) comparing to UV light irradiation (Fig. 18 on page 47). This may be due to a different stock of NCS that was order for experiments with HeLa and RPE cells.

Interestingly, the results showed no significant difference in the amount of γH2AX in HeLa cells (Fig. 26 on page 55), neither in RPE cells (Fig. 27 on page 56) for Prpf8 KD comparing to the negative control. These findings indicate that the Prpf8 protein is not involved in ATM DDR pathway that is activated after NCS treatment. Previously, it was shown that however Prpf8 protein undergoes phosphorylation after ionizing radiation, no such an event was detected after NCS treatment.[85] [85] This supports our conclusion that the involvement of Prpf8 protein in DDR is depend on a type of DNA damage.

6 Conclusion

The main aim of this diploma thesis was to investigate the involvement of Prpf8 protein in cellular response to DNA damage.

We found that the Prpf8 protein is important for the ATR DNA damage response pathway, which is activated after the UV light irradiation. Cells with reduced expression of Prpf8 protein showed disability to repair the DNA lesions after the UV light treatment. We also observed differences in cellular response to UV light irradiation in different RP mutated cell lines. Unfortunately, the results were not significant therefore another experiments are needed to confirm that the Prpf8-S2118F mutant is not able to rescue the down regulation of exogenous Prpf8 protein, in contrast to Prpf8-Y2334 mutant that showed similar phenotype as the Prpf8-WT and rescued the KD of Prpf8 protein.

Surprisingly, we did not observe any differences in cellular response to DNA damage caused by NCS treatment after the down regulation of the Prpf8 protein, suggesting that the protein is not involved in the ATM DNA damage response pathway.

7 References

1. Alberts, B., Johnson, A., Lewis, J., Raff, M., Roberts & K. Walter, P. *Molecular Biology of the Cell*. (Garland Science, 5th edition, 2008).
2. Lander, E. S., Linton, L. M., Birren, B., Nusbaum, C., Zody, M. C., Baldwin, J., Devon, K., Dewar, K., Doyle, M., FitzHugh, W., Funke, R. & *et al.* Initial sequencing and analysis of the human genome. *Nature* **409,** 860–921 (2001).
3. Cvitkovic, I., Jurica & M. S. Spliceosome database: A tool for tracking components of the spliceosome. *Nucleic Acids Res.* **41,** 132–141 (2013).
4. Turunen, J. J., Niemelä, E. H., Verma, B. & Frilander, M. J. The significant other: Splicing by the minor spliceosome. *Wiley Interdiscip. Rev. RNA* **4,** 61–76 (2013).
5. Wongpalee, P. S. & Sharma, S. The pre-mRNA splicing reaction in *Spliceosomal Pre-mRNA Splicicng* (Hertel, J. K., Springer Dordrecht Heidelberg, London, New York, 2014, pp. 45-53).
6. Crooks, G., Hon, G., Chandonia, J. & Brenner, S. WebLogo: a sequence logo generator. *Genome Res.* **14,** 1188–1190 (2004).
7. Mater, A. G., Wang, Z. A day in the life of the spliceosome. *Nat. Rev. Mol. Cell Biol.* **15,** 108–121 (2014).
8. Matlin, J. A., Clark, F. & Smith, J. W. S. Understanding alternative splicicng: towards a cellular code. *Nat. Rev. Mol. Cell Biol.* **6,** 386–398 (2005).
9. Wagner, D. S. & Berglund, J. A. Alternative pre-mRNA splicing in *Spliceosomal Pre-mRNA Splicicng* (Hertel, J. K., Springer Dordrecht Heidelberg, London, New York, pp. 45-55).
10. Cartegni, L., Chew, L. S. & Krainer, R. A. Listening to silence and understanding nonsense: exonic mutations that affect splicing. *Nat. Rev. Genet.* **3,** 285–298 (2002).
11. Lee, Y. & Rio, D. C. Mechanisms and regulation of alternative pre-mRNA splicing. *Annu.Rev.Biochem.* **84,** 291–323 (2015).
12. Weinberg, A. R. & Penman, S. Small molecular weight monodisperse nuclear RNA. *J. Mol. Biol.* **38,** 289–304 (1968).
13. Wahl, M. C. & Fischer, U. The right pick: Structural basis of snRNA selection by Gemin5. *Genes Dev.* **30,** 2341–2344 (2016).
14. Staněk, D., Rader, S. D., Klingauf, M. & Neugebauer, K. M. Targeting of U4/U6 small nuclear RNP assembly factor SART3/p110 to Cajal bodies. *J. Cell Biol.* **160,**

505–516 (2003).

15. Staněk, D. & Neugebauer, K. M. The Cajal body: a meeting place for spliceosomal snRNPs in the nuclear maze. *Chromosoma* **115,** 343–354 (2006).
16. Wahl, M. C., Will, C. L. & Lührmann, R. The Spliceosome: Design principles of a dynamic RNP machine. *Cell* **136,** 701–718 (2009).
17. Will, C. L. & Lührmann, R. Spliceosome structure and function. *Cold Spring Harb. Perspect. Biol.* **3,** 1–23 (2011).
18. Malinova, A. The role of pre-mRNA splicing in human hereditary diseases. Doctoral Thesis, Study program: Molecular and cellular biology, genetics and virology, Faculty of Science, Charles University (2017).
19. Bach, M., Winkelmann, G. & Lührmann, R. 20S small nuclear ribonucleoprotein U5 shows a surprisingly complex protein composition. *Proc. Natl. Acad. Sci. U. S. A.* **86,** 6038–42 (1989).
20. Nguyen, D. H. T., Galej., P. W., Bail, X., Sayva, G. Ch., Newman, J. A., Scheres, W. H. S. & Nagai, K. The architecture of the spliceosomal U4/U6.U5 tri-snRNP. *Nature* **523,** 47–52 (2015).
21. Newman, A. J. The role of U5 snRNP in pre-mRNA splicing. *EMBO J.* **16,** 5797–5800 (1997).
22. Jackson, S. P., Lossky, M. & Beggs, J. D. Cloning of the RNA8 gene of Saccharomyces cerevisiae, detection of the RNA8 protein, and demonstration that it is essential for nuclear pre-mRNA splicing. *Mol. Cell. Biol.* **8,** 1067–1075 (1988).
23. Agafonov, D. E., Kastner, B., Dybkov, O., Hofele, R. V., Liu, W., Urblaub, H., Luhrmann, R. & Stark, H. Molecular architecture of the human U4/U6.U5 tri-snRNP. *Science* **351,** 1416–1420 (2016).
24. Grainger, R. J. Prp8 protein: At the heart of the spliceosome. *RNA* **11,** 533–557 (2005).
25. Vincent, M. *et al.* The nuclear matrix protein P255 is a highly phorphorylated form of RNA polymerase II largest subunit which associates with spliceosomes. *Nucleic Acids Res.* **24,** 4649–4652 (1996).
26. Galej, W. P., Oubridge, C., Newman, A. J. & Nagai, K. Crystal structure of Prp8 reveals active site cavity of the spliceosome. *Nature* **493,** 638–643 (2013).
27. Faustino, N. A., Cooper, T. a & Andre, N. Pre-mRNA splicing and human disease. *Genes Dev.* **17,** 419–437 (2003).

28. Krawczak, M., Reiss, J. & N., C. D. The mutational spectrum of single base- pair substitutions in mRNA splice junctions of human genes: causes and consequences. *Hum. Genet.* **90,** 41–54 (1992).
29. Klamt, B., Koziell, A., Poulat, F., Wieacker, P., Scambler, P., Berta, P. & Gessler, M.,Frasier syndrome is caused by defective alternative splicing of WT1 leading to an altered ratio of WT1 +/-KTS splice isoforms. *Hum. Mol. Genet.* **7,** 709–714 (1998).
30. David, C. J. & Manley, J. L. Alternative pre-mRNA splicing regulation in cancer: Pathways and programs unhinged. *Genes Dev.* **24,** 2343–2364 (2010).
31. Lefebvre, S., Bürglen, L., Clermount, O., Burlet, P., Viollet, L., Benichou, B., Cruaud, C., Millasseau, P., Zeviani, M., Le Paslier, D., Frézal, J., Cohen, D., Weissenbach, J., Munnich, A. & Melki, J. Identification and characterization of a spinal muscular atrophy-determining gene. *Cell* **80,** 155–165 (1995).
32. Talbot, K. & Davies, E. K. Spinal muscular atrophy. *Semin Neurol* **21,** 189–198 (2001).
33. Nlend Nlend, R., Meyer, K. & Schümperli, D. Repair of pre-mRNA splicing: Prospects for a therapy for spinal muscular atrophy. *RNA Biol.* **7,** 430–440 (2010).
34. Hamel, C. Retinitis pigmentosa. *Orphanet J. Rare Dis.* **1,** 1–12 (2006).
35. Hartong, T. D., Berson, L.-E. & Dryja, P. T. Retinitis Pigmentosa. *Lancet* **368,** 1795–1809 (2006).
36. Mordes, D., Luo, X., Kar, A., Kuo, D., Xu, L., Fushimi, K., Yu, G., Sternberg, P. & Wu, J. Pre-mRNA splicing and retinitis pigmentosa. *Mol. Vis.* **12,** 1259–71 (2006).
37. Cvačková, Z., Matějů, D. & Staněk, D. Retinitis pigmentosa mutations of SNRNP200 enhance cryptic splice-site Recognition. *Hum. Mutat.* **35,** 308–317 (2014).
38. Pena, V., Liu, S., Bujnicki, J. M., Lührmann, R. & Wahl, M. C. Structure of a multipartite protein-protein interaction domain in splicing factor Prp8 and its link to retinitis pigmentosa. *Mol. Cell* **25,** 615–624 (2007).
39. Mozaffari-Jovin, S., Wandersleben, T., Santos, F. K., Will, L. C., Luhrmann, R. & Wahl, C. M. Inhibition of RNA helicase Brr2 by the C-Terminal tail of the spliceosomal protein Prp8. *Science* **341,** 80–84 (2013).
40. Maeder, C., Kutach, A. K. & Guthrie, C. ATP-dependent unwiding of U4/U6 snRNAs by the Brr2 helicase requires the C-terminus of Prp8. *Nat. Struct. Mol.*

Biol. **16,** 42–48 (2009).

41. Mozaffari-Jovin, S., Wandersleben, T., Santos, K. F., Will, C. L. & Wahl, M. C. Novel regulatory principles of the spliceosomal Brr2 RNA helicase and links to retina disease in humans. *RNA Biol.* **11,** 298–312 (2014).
42. Towns, V. K., Kipioti, A., Long, V., McKibbin, M., Maubaret, C., Vaclavik, V. & Ehsani, P. Prognosis for splicing factor PRPF8 retinitis pigmentosa, novel mutations and correlation between human and yeast phenotypes. *Hum. Mutat.* **31,** 1361–1376 (2010).
43. Malinová, A., Cvačková, Z., Matějů, D., Hořejší, Z., Abéza, C., Vandermoere, F., Bertrand, E., Satněk, D. & Verheggen, C. Assembly of the U5 snRNP component PRPF8 is controlled by the HSP90/R2TP chaperones. *J. Cell Biol.* **216,** 1579–1596 (2017).
44. Růžičková, Š. & Staněk, D. Mutations in spliceosomal proteins and retina degeneration. *RNA Biol.* **14,** 544–552 (2016).
45. Annunziato, A. DNA Packing: Nucleosomes and Chromatin. *Nature Education* https://www.nature.com/scitable/topicpage/dna-packaging-nucleosomes-and-chromatin-310, (2008).
46. Kornberg, R. Structure of chromatin. *Annu. Rev. Biochem.* **46,** 954–965 (1977).
47. Epigenetic Group. A detailed guide to histone modifications investigated in epigenetic research, https://www.epigentek.com/catalog/advanced-epigenetic-overview-of-histone-modifications-n-5.html, (2017).
48. Allfrey, G., Faulkner, R. & Mirsky, A. E. Possible role in the regulation of RNA synthesis. *Proc. Natl. Acad. Sci. U. S. A.* **315,** 786–794 (1964).
49. David, M., Macalpine, D. M. & Almouzni, G. Chromatin and DNA replication. *Cold Spring Harb Perspect Biol* **5,** 1-22 (2013).
50. Maréchal, A. & Zou, L. DNA Damage Sensing by the ATM and ATR kinases. *Cold Spring Harb Perspect Biol* **5,** 1–18 (2013).
51. Zhou, B.-B. S. & Elledge, S. S. The DNA damage response: putting checkpoints in perspective. *Nature* **408,** 433–439 (2000).
52. Bannister, A. J. & Kouzarides, T. Regulation of chromatin by histone modifications. *Cell Res.* **21,** 381–395 (2011).
53. Rossetto, D., Avvakumov, N. & Coté, J. Histone phosphorylation: A chromatin modification involved in diverse nuclear events. *Epigenetics* **7,** 1098–1108 (2012).

54. Rodríguez-Paredes, M. & Esteller, M. Cancer epigenetics reaches mainstream oncology. *Nat. Med.* **17,** 330–339 (2011).
55. Marzluff, W. F., Gongidi, P., Woods, K. R., Jin, J. & Maltais, L. J. The human and mouse replication-dependent histone genes. *Genomics* **80,** 487–498 (2002).
56. Bönisch, C. & Hake, S. B. Histone H2A variants in nucleosomes and chromatin: More or less stable? *Nucleic Acids Res.* **40,** 10719–10741 (2012).
57. Rogakou, E., Boon, C., Redon, C. & Bonner, W. Megabase Chromatin domains involved in DNA double-strand breaks in vivo. *J. Cell Biol.* **146,** 905–915 (1999).
58. Attikum, H. & Gasser, S. M. The histone code at DNA breaks: a guide to repair? *Nat. Rev. Mol. Cell Biol.* **6,** 757–765 (2005).
59. Brown, E. J. & Baltimore, D. ATR disruption leads to chromosomal fragmentation and early embryonic lethality. *Genes Dev.* **14,** 397–402 (2000).
60. Zou, L. & Elledge, S. J. Sensing DNA Damage Through ATRIP Recognition of RPA-ssDNA Complexes. *Science.* **300,** 1542–1548 (2003).
61. Shiotani, B., & Zou, L. Single-stranded DNA orchestrates an ATM-to-ATR switch at DNA breaks. *Mol. Cell.* **33,** 547-558 (2009).
62. Banerjee, T. & Chakravarti, D. A peek into the complex realm of histone phosphorylation. *Mol. Cell. Biol.* **31,** 4858–4873 (2011).
63. Shiloh, Y. ATM and related protein kinases: safeguarding genome integrity. *Nat. Rev. Cancer* **3,** 155–168 (2003).
64. Awasthi, P., Foiani, M. & Kumar, A. ATM and ATR signaling at a glance. *J. Cell Sci.* **129,** 1285–1285 (2016).
65. Broustas, C. G. & Lieberman, H. B. DNA damage response genes and the development of cancer metastasis. *Radiat. Res.* **181,** 111–130 (2014).
66. Krokan, H. E. & Bjoras, M. Base excision repair. *Cold Spring Harb. Perspect. Biol.* **5,** 1-22 (2013).
67. Lindahl, T. Instability and decay of the primary structure of DNA. *Nature* **362,** 709–715 (1993).
68. Hoeijmakers, J. Genome maintenance mechanism for preventing cancer. *Nat. Rev. Mol. Cell Biol.* **411,** 366–374 (2001).
69. Sugasawa, K. Regulation of damage recognition in mammalian global genomic nucleotide excision repair, *Mutat. Res.* **685,** 29–37 (2009).
70. Jiricny, J. The multifaceted mismatch-repair system. *Nat. Rev. Mol. Cell Biol.* **7,**

335–346 (2006).

71. Li, G.-M. Mechanisms and functions of DNA mismatch repair. *Cell Res.* **18,** 85–98 (2008).

72. Dexheimer, T. S. DNA repair pathways and mechanisms in *DNA repair of cancer stem cells* (Mathews, L., Cabarcas, S., Hurt, E., Springer, Dordrecht, 2013, pp. 19-32).

73. Haber, J. E. Partners and pathways repairing a double-strand break. *Trends Genet.* **16,** 476–479 (2000).

74. Sung, P. & Klein, H. Mechanism of homologous recombination: Mediators and helicases take on regulatory functions. *Nat. Rev. Mol. Cell Biol.* **7,** 739–750 (2006).

75. Lieber, M. R. The Mechanism of Double-Strand DNA Break Repair by the Nonhomologous DNA End Joining Pathway. *Annual Review of Biochemistry* **79,** 181-211 (2011).

76. Mao, Z., Bozzella, M., Seluanov, A. & Gorbunova, V. Comparison of nonhomologous end joining and homologous recombination in human cells. *DNA Repair.* **7,** 1765–1771 (2009).

77. Yasui, A. & McCready, S. J. Alternative repair pathways for UV-induced DNA damage. *BioEssays* **20,** 291–297 (1998).

78. Goldber, I. H. Mechanism of neocarzinostatin action: role of DNA microstructure in determination of chemistry of bistranded oxidative damage. *Acc. Chem. Res.* **24,** 191–198 (1991).

79. Vrouwe, M. G., Pines, A., Overmeer, R. M., Hanada, K. & Mullenders, L. H. F. UV-induced photolesions elicit ATR-kinase-dependent signaling in non-cycling cells through nucleotide excision repair-dependent and -independent pathways. *J. Cell Sci.* **124,** 435–46 (2011).

80. Povirk, LF. DNA damage and mutagenesis by radiomimetic DNA-cleaving agents: bleomycin, neocarzinostatin and other enediynes. *Mutat. Res.* **355,** 71–89 (1996).

81. Patil, M., Pabla, N. & Dong, Z. Checkpoint kinase 1 in DNA damage response and cell cycle regulation. *Cell Mol. Life Sci.* **70,** 4009–4021 (2013).

82. White, D. E., Ivanov, A. V, Corsinotti, A., Peng, H. & Lee, S. C. The ATM substrate KAP1 controls DNA repair in heterochromatin : Regulation by HP1 proteins and Serine 473/824 phosphorylation. *Mol. Cancer Res.* **10,** 401–414 (2012).

83. Shkreta, L. & Chabot, B. The RNA splicing response to DNA damage.

Biomolecules **5,** 2935–2977 (2015).

84. Harada, A., Matsuzaki, K., Takeiri, A. & Mishima, M. The predominant role of apoptosis in γH2AX formation induced by aneugens is useful for distinguishing anegens from clastrogens. *Mutat. Res. - Genet. Toxicol. Environ. Mutagen.* **771,** 23–29 (2014).

85. Bensimon, A., Schmidt, A., Ziv, Y., Elkon, R. & Chen, D. J. ATM-Dependent and Independent Dynamics of the Nucleat Phosphoproteome After DNA Damage. *Sci. Signal.* **3,** (2010).

Svoluji k zapůjčení této práce pro studijní účely a prosím, aby byla řádně vedena evidence vypůjčovatelů.

Jméno a přijímení s adresou	Číslo OP	Datum vypůjčení	Poznámky